Pliocene climate change on Ellesmere Island, Canada: annual variability determined from stable isotopes of fossil wood

Submitted to the College of Graduate Studies & Research
in partial fulfillment of the requirements
for the degree of Master of Science
June, 2006 at the
Department of Geological Sciences,
University of Saskatchewan, Saskatoon, Saskatchewan, S7N 5E2

Adam Zoltan Csank

Permission to use

In presenting this thesis in partial fulfillment of the requirements for a Postgraduate degree from the University of Saskatchewan, I, Adam Zoltan Csank, agree that the Libraries of this University may make it freely available for inspection. I further agree that permission for copying of this thesis in manner, in whole or in part, for scholarly purposes may be granted by myself, Dr. James F. Basinger or Dr. William P. Patterson and in my, or the aforementioned individuals absence, by the Head of the Department of Geological Sciences or the Dean of the College of Graduate Studies. It is understood that any copying or publication or use of this thesis or parts thereof for financial gain shall not be allowed without written permission of the author. It is also understood that due recognition shall be given to the author and to the University of Saskatchewan in any use which may be made of any material in the thesis entitled *Pliocene climate change on Ellesmere Island, Canada: annual variability determined from stable isotopes of fossil wood*.

Requests for permission to copy or to make any use of material in this thesis in whole or part shall be addressed to Adam Zoltan Csank or to:

Head of the Department of Geological Sciences
University of Saskatchewan,
Saskatoon, Saskatchewan, S7N 5E2, Canada

University of Saskatchewan
College of Graduate Studies and Research

Abstract

Submitted in partial fulfillment
of the requirements of the

Degree of Master of Science

by

Adam Zoltan Csank

Department of Geological Sciences,
University of Saskatchewan
Spring, 2006

Examining Committee:

Dr. K. Ansdell	Chair of Graduate Committee
Dr. J. Basinger	Co-Supervisor, Department of Geological Sciences
Dr. W. Patterson	Co-Supervisor, Department of Geological Sciences
Dr. H. Cota-Sánchez	Department of Biology
Dr. C. Holmden	Department of Geological Sciences
Dr. R. Renaut	Department of Geological Sciences
Dr. J. Romo	External Reviewer, Department of Plant Sciences

Pliocene climate change on Ellesmere Island, Canada: Annual variability determined from stable isotopes of fossil wood

Tree-ring analyses have contributed significantly to investigations of climate change and climate cycles, including the North Atlantic Oscillation (NAO), Pacific Decadal Oscillation (PDO) and El Niño/Southern Oscillation (ENSO). Stable isotope climate proxies ($\delta^{18}O$, δD, and $\delta^{13}C$) have enhanced traditional ring-width data, although poor preservation of ancient wood has generally constrained reconstruction of stable isotope proxy records to the Holocene and Late Pleistocene. An opportunity to apply these stable isotope methods to older wood has been presented by recovery of remains of Mixed-

Coniferous Boreal Vegetation, in Early Pliocene (4-5 Ma) deposits at Strathcona Fiord, Ellesmere Island, Canada (~79°N). An exceptionally well-preserved tree trunk, identified as *Larix* (larch) through wood anatomical characteristics, from this high Arctic site provided a 203-year tree-ring record, from which we present the first high-resolution, secular isotope record of Pliocene climate. $\delta^{18}O$, δD, and $\delta^{13}C$ isotope values indicate a variable climate with alternating intervals of cool/wet to warm/dry weather. These fluctuations in climate may be attributable to phase changes in climate cycles observed in the record. A growing season mean temperature of 14.4 °C was calculated from isotopic analysis of gastropod shells. Palaeoclimatic modeling of tree isotope values has revealed growing season temperatures of 11-15 °C, and estimated isotope values of precipitation of –18.3 ‰ ($\delta^{18}O$) and –228 ‰ (δD). Both palaeotemperature estimates and source water calculations are comparable to those found in a modern Boreal Forest. Time-series wavelet analysis was applied to these data revealing prominent short (<10 years), intermediate (16-35 years) and long-term (~45-50 years) cyclicity. These are the highest resolution climate cycles recovered from the pre-Holocene terrestrial record, providing evidence for decadal scale cyclicity similar to the NAO and/or PDO 4-5 million years ago.

Acknowledgements

This thesis would not have been possible without the help of the people mentioned bellow. Their guidance, support, instruction and encouragement made this project possible.

- My supervisors Dr. James Basinger and Dr. William Patterson
- Tim Prokopiuk and Aaron Diefendorf for their laboratory assistance
- Dr. Bruce Eglington for his assistance with the wavelet analysis
- Dr. A. Davis for use of his microtome and paraffin for wood sectioning
- Dr. Hugo Cota-Sanchez, Dr. Susan Kaminskyj and Andrew Postinikoff for field assistance.
- Justin Dodd for valuable discussions and helpful comments.
- Funding from the Geological Society of America Graduate student research grant # 7637-04, the Northern Scientific Training Program, NSERC Discovery grants # 1334-98 to Dr. James Basinger and # 261623-03 to Dr. William Patterson are also gratefully acknowledged.
- I would also like to thank Aaron Diefendorf, Kristin Dietrich, Justin Dodd, Elise Dufour, Dan LaPorte, Kyle McMillan and Antoine Zazzo for their friendship throughout my time here, you guys kept me sane.

Table of Contents

List of Tables

List of Figures

List of Abbreviations

AO: Arctic Oscillation
CN: Cellulose Nitrate
CNIP: Canadian Network for Isotopes in Precipitation
DSDP: Deep Sea Drilling Program
EA: Elemental Analyzer
ENSO: El Niño/Southern Oscillation
Ma: Million annums
NADW: North Atlantic Deep Water
NAO: North Atlantic Oscillation
NWT: Northwest Territories
ODP: Ocean Drilling Project
PDO: Pacific Decadal Oscillation
RH: Relative Humidity
RH-T: Relative Humidity – Temperature
RLS: Radial Section
SST: Sea Surface Temperatures
SW: Source Water
TC/EA: High Temperature Conversion Elemental Analyzer
TLS: Tangential Section
TS: Transverse Section
VPDB: Vienna Pee-Dee Belemnite
VSMOW: Vienna Standard Mean Ocean Water
YT: Yukon Territory

1. Introduction

Throughout much of the Mesozoic and Cenozoic, the Earth experienced a warmer "greenhouse" phase of climate than is present in the modern. One of the most intriguing facets of these periods is that vast forests grew at latitudes as high as 82° N and 75° S (Spicer and Chapman, 1990). These forests persisted well above the current extent of the modern tree line and trees would have had to survive dark winters and periods of continuous light in summer, conditions that made these polar forests biomes without any close modern analogues.

Beginning in the 1850s the Earth has undergone a period of 'anthropogenically-forced global warming'. From the start of the industrial revolution atmospheric CO_2 has undergone a 30% increase (from 280 ppm to 371 ppm) (Keeling and Whorf, 2005). Recent predictions indicate that if current emissions are maintained, the concentration of atmospheric CO_2, will double by the year 2100 (Keeling and Whorf, 2005). Given the relationship between temperature and CO_2 concentration, this doubling of CO_2 concentration could increase temperatures by as much as 11°C (Stainforth *et al*., 2005).

In recent decades, the response of high-latitudes to changes in climate has lead to renewed interest in the study of ancient ecosystems under greenhouse conditions. Well preserved wood, examined in this study, affords the opportunity to conduct the first multi-proxy, high-resolution study of Early Pliocene climate and variability. A stable isotope study of tree-rings was possible using an Early Pliocene log collected on Ellesmere Island, Canada. Recently, the Early Pliocene has been proposed as an analogue for future climate should current warming continue (Haywood and Valdes, 2004). It is

thus important to understand this critical period if we are to understand what may occur in the future, after all the past is the key to the future.

1.1 Aims and Objectives

This study utilizes multi-proxy, stable isotope analyses of a Pliocene log from Ellesmere Island, Canada to address three major questions: (1) What were the climatic conditions on Ellesmere Island during the Early Pliocene? (2) How did these climatic conditions vary on an annual basis? Studies of modern climate cycles have revealed the strong influence that cycles such as El Nino/Southern Oscillation (ENSO), the North Atlantic Oscillation (NAO) and most recently the Pacific Decadal Oscillation (PDO) have on climate and climate changes (Briffa, 2000; Cook, 2001; Moritz *et al*., 2005). Thus the final question is: (3) Is there evidence for decadal scale climate cycles, such as ENSO, NAO and PDO in the Early Pliocene? The first objective was to obtain oxygen, carbon and hydrogen isotope records with annual resolution from tree rings of an Early Pliocene log from Ellesmere Island. The second objective was to use the isotope records to provide insight into Pliocene terrestrial climate, and the final objective was to use time-series wavelet analysis to identify and investigate climate variability, specifically cycles in the tree-ring and isotope records.

1.2 Late Tertiary Arctic palaeoclimate: An overview

The Eocene was the last period when the Earth was in a true greenhouse phase of climate (Dowsett *et al.*, 1996). The Eocene-Oligocene boundary is marked by a shift from

a greenhouse climate to an icehouse climate. This shift was originally interpreted to reflect a decrease in mean annual temperature, though no supporting information could be found. Subsequently the shift in climate has been related to increasing seasonality in temperature (Ivany *et al*., 2000). High-latitude temperature and precipitation patterns are particularly sensitive to global climatic conditions (Overpeck *et al*., 1997). Characterization of polar climates during past warm periods allows better understanding of future greenhouse climate dynamics. In addition, the study of polar climates immediately prior to the onset of glaciation is crucial for our understanding of the conditions that lead to the Ice Ages.

During the Eocene, Australia, Antarctica, and South America were joined together as Gondwana, while North America and Asia were periodically connected by the Bering land bridge (Berggren and Prothero, 1992). As such, Arctic and Antarctic Ocean circulation were considerably different than today. Deep-water circulation was restricted by lack of a Trans-Antarctic current, while cross latitude circulation was enhanced (Diester-Haass and Zahn, 1996). The lack of these isolating currents is believed to be the primary cause of the warmer temperatures, because warm water from the equator would have reached both poles.

Although marine organic matter and pedogenic carbonate indicate CO_2 levels in the Eocene were as high as 1000-1500 ppm (Ekart *et al.,* 1999; Pagani *et al*., 2005) it has been shown that Pliocene atmospheric CO_2 was not significantly higher than today (Raymo *et al.*, 1996; Ekart *et al*., 1999; Royer *et al*., 2001) indicating that CO_2 was not a major factor contributing to warmer temperatures. After determining sea water $\delta^{18}O$ values increased from 0.2‰ to 1.8‰VPDB in the Pliocene, surface water estimates are

closer to ~2˚C warmer than today (Zachos *et al.,* 2001; Williams *et al*., 2005). By the end of the Eocene, the opening of the Drake Passage and the separation of Australia from Antarctica resulted in the formation of the Trans-Antarctic current, completing the isolation of Antarctica (Diester-Haass and Zahn, 1996). The isolation and cooling of Antarctica provided for the formation of cool dense Antarctic bottom water which began to drive deep-water circulation, increasing the transfer of cool water into lower latitudes (Zachos *et al*., 2001).

Based on evidence from marine $\delta^{18}O$ records of benthic foraminifera glaciation in the Northern Hemisphere is believed to have started in the late Miocene (Maslin *et al*., 1996). However, the first evidence of major ice sheets in the Northern Hemisphere was not until 2.55 million years ago in the late Pliocene (Shackleton *et al*., 1984). Formation of these ice sheets is believed to be the culmination of a larger scale Pliocene cooling event that started earlier, at ~3.2 Ma (Maslin *et al*., 1996; Tiedemann *et al*., 1994).

The Pliocene is the last period of time in which a warmer-than-present climate existed for an extended period (Dowsett *et al*. 1996). What makes the Pliocene truly intriguing is that many of the factors that regulate climate were similar to modern day. Stomatal density studies suggest that CO_2 concentrations were not significantly greater than they have been in the last 200 years (Kurschtner *et al*., 1996), An increase in atmospheric CO_2 concentration may lead to a decrease in the number of leaf stomata in some taxa (Van Der Burgh *et al*., 1993). $\delta^{13}C$ ratios of marine organic matter, also a proxy for atmospheric CO_2, confirms that CO_2 concentrations were at most an average of ~35% greater than the pre-industrial concentration of 280 ppm (Raymo *et al*., 1996). Reduced thermohaline circulation, due to less dense northern water combined with a

northern flow of warm water from the equator would have increased heat transfer to the Arctic, as the Arctic Ocean may not have been cold enough to send a countering cool water current south (Haywood *et al.* 2000; Edwards *et al.* 1991). Recently Haywood and Valdes (2004) suggested that the lack of polar ice cover during the Pliocene would have caused a strong albedo feedback, warming the poles significantly.

The onset of Northern Hemisphere glaciations began with stepwise cooling starting at 3.5 Ma and culminating at 2.5 Ma, with first appearance of a Greenland ice sheet at ~3.3 Ma and expansion of the Greenland, Scandinavian and Arctic ice sheets from 2.75 Ma on (Flesche Kleiven *et al*., 2002; Haywood *et al*., 2002). North Atlantic Deep Water (NADW) records from Iceland indicate significant changes in NADW production parallel the cooling trend from 3.3 Ma (Flesche Kleiven *et al*., 2002). The mid-Pliocene, ~3 Ma, is particularly interesting as this period had several rapid cooling events such as the MG2 (3.35 Ma), M2 (3.31 Ma), KM2 (3.12 Ma) and G20 (3.01 Ma) isotope excursions recorded in the oxygen isotopes of Benthic foraminifera (Shackelton *et al.* 1995). $\delta^{18}O$ records from the North Pacific show a warming of ~4° C in sea surface temperatures during the approximately 80 ka before the expansion of the ice sheets, perhaps related to changes in ocean circulation (Maslin *et al.*, 1996). The warm water would have provided a source of moisture providing the precipitation necessary to form the ice sheets in the Arctic and in Greenland. At around 2.7 Ma there was rapid cooling in the north as indicated by an abrupt drop of 7.5 °C in North Pacific sea-surface temperatures (Maslin *et al*., 1996), an increase in ice-rafted debris in the North Atlantic (Flesche Kleiven *et al*., 2002) and increases in benthic foraminiferal $\delta^{18}O$ values (Tiedemann *et al*., 1994; Shackleton *et al*., 1995). This event seems to be related to a

reduction in thermohaline circulation and NADW production, although the causes of this reduction are much debated (Maslin *et al*., 1996). Figure 1.2.1 presents a deep-sea stable isotope record for the Tertiary, illustrating the major cooling events that began in the Oligocene and culminated with the glaciation of the Northern Hemisphere in the Pliocene.

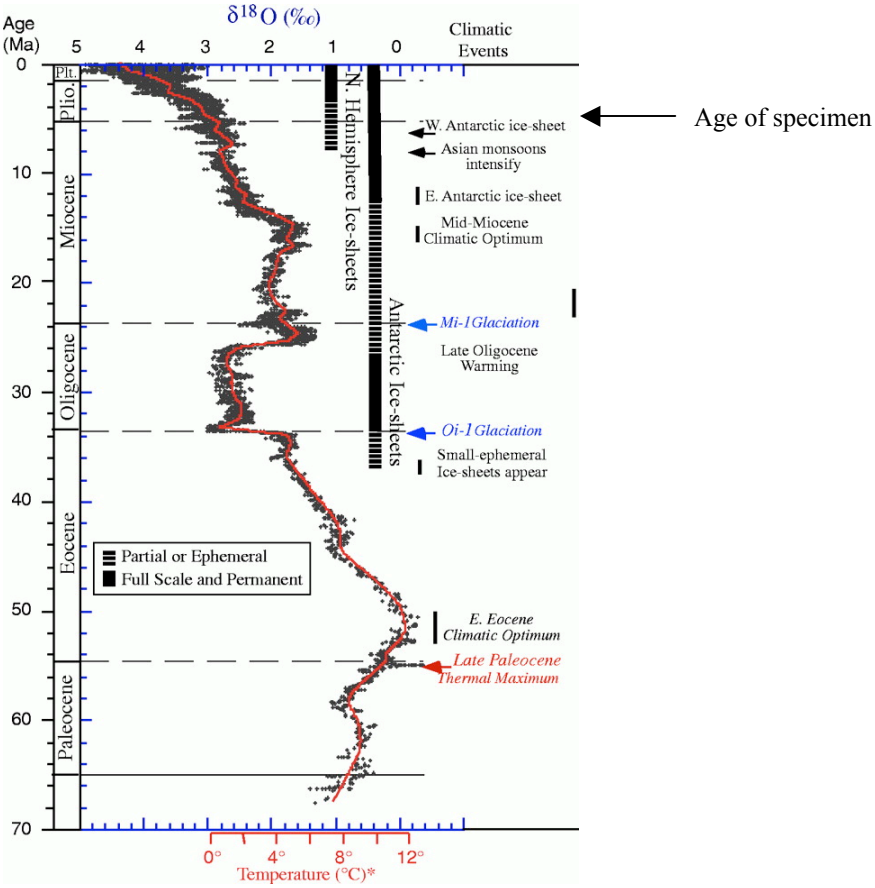

Figure 1.2.1: Global deep-sea stable isotope record of the Tertiary, compiled from DSDP (Deep Sea Drilling Program) and ODP (Ocean Drilling Project) records. Periods of Antarctic and North American Ice Sheet formation are indicated to the right as well as several major climatic events. Temperature is indicated as a red line (adapted from Zachos *et al*., 2001).

1.3 Polar Forests: An extinct biome

One of the most intriguing facets of the Earths warm phases were the forests present at both poles. Rich Pliocene fossil floras have been described from Alaska (Matthews and Ovenden, 1990), Antarctica (Francis and Hill, 1996; van Bergen and Poole, 2002), Siberia (Demske *et al*., 2002), Greenland (Funder *et al*., 2001; Bennike *et al*., 2002) and Arctic Canada (Matthews and Ovenden, 1990; Fyles *et al*., 1998; Tedford and Harington, 2003) all located well above the Pliocene polar circles (Fig. 1.3.1). Forests existed at palaeolatitudes ranging from 66-82°. The most northerly modern forest is at Ary-Mas (72° N) in Northern Russia, and the most southerly tree-line is at 59° N in Northern Quebec.

The Eocene High Arctic consisted of lush vegetation dominated by warm adapted conifer species that currently only exist in the forests of southern China (McIver and Basinger, 1999). This vegetation continued to thrive as an ecosystem until terminal Eocene cooling produced a shift to more boreal vegetation.

Flora from the well known 'Beaver Pond' locality near Strathcona Fiord on Ellesmere Island, dated at 4-5 Ma, consisted of *Betula* (birch), *Larix* (larch), *Picea* (spruce) as well as abundant mosses and ferns that are all characteristic of boreal (taiga) flora (Tedford and Harington, 2003).

Records from Meighen Island in the Canadian Arctic, dated to about 3 Ma, show a mixture of Arctic and Boreal vegetation (Matthews and Ovenden, 1990). Palynological records from the Hvitland beds on Ellesmere Island, dated at around 2.5 Ma, show exclusively tundra vegetation (Fyles *et al*., 1998) indicating that by this time the polar forests had disappeared.

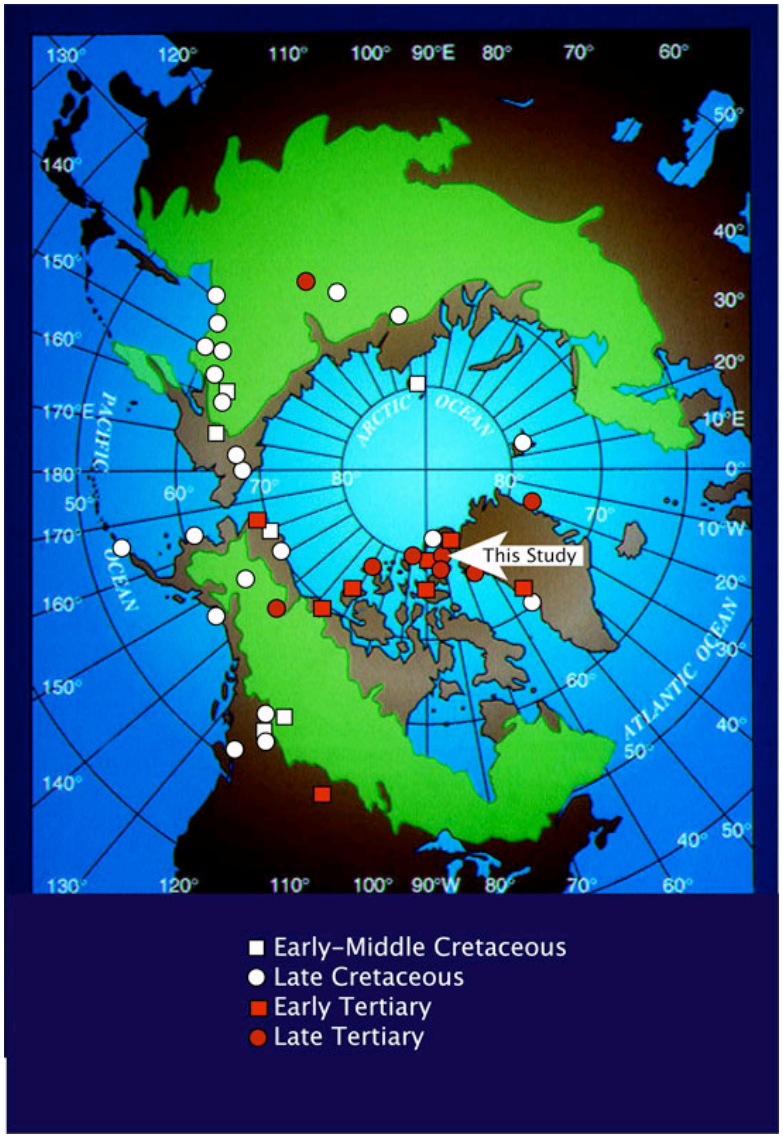

Figure 1.3.1: Polar map depicting selected fossil forest sites and showing the extent of the modern boreal forest in green. The present study is indicated by an arrow (adapted from Hare and Ritchie, 1972).

2. Stable isotopes and tree-rings as palaeoclimate proxies

Dendroclimatology has proven extremely useful in extending our knowledge of climate to periods prior to establishment of instrumental records. Tree-ring widths can be used to indicate growing conditions, including various climatic and ecological factors such as, temperature, water, irradiance, soil nutrients and stand density. Depending on the environment, different ecological factors may dominate. For example tree-ring widths depend on the amount of water available to a tree during the growing season in an arid environment or a tundra where water is scarce (Creber, 1977). However, it is difficult to determine which of the myriad of parameters is causing the variation in tree growth unless specific site conditions are known.

Determination of $\delta^{18}O$, $\delta^{13}C$ and δD isotope values of wood cellulose is a valuable method for recovering palaeoclimate information from the Holocene and Late Pleistocene (e.g. McCarroll and Loader, 2004). Epstein and Yapp (1976) determined δD values for a 1000-year period from a Kauri tree from New Zealand and found a correlation between isotope values and the 50-year moving average of the temperature record. Given the large number of well known dendrochronological records, such as the bog oak of the British Isles (Baillie *et al.*, 2000) and the Tasmanian Huon pine record (Cook *et al*., 2000) among many others (i.e. Creber, 1977; Creber and Chaloner, 1985; Briffa, 2000; Baillie *et al.*, 2000; Cook *et al.*, 2002; D'Arrigo *et al*., 2005) it soon became apparent that there was a treasure trove of untapped information. For example, in parts of Europe there are tree ring chronologies that extend back as far as 9,200 years (Baillie *et*

al., 2000). However, poor preservation of ancient wood has generally limited the use of this method. Studies of pre-modern wood have required preservation such that cellulose has not become degraded by microbial action, thereby limiting these studies to samples from preservational situations such as peat bogs or anoxic lake sediments. Two recent studies examined well-preserved Tertiary woods from the Arctic and Antarctic using stable isotopes, proving that with good preservation it is possible to extract stable isotope values from pre-Quaternary wood (Jahren and Sternberg, 2003; van Bergen and Poole, 2002).

2.1 Water Isotopes: Oxygen and Hydrogen

Cellulose is composed of carbon, oxygen and hydrogen in the ratio $C_6H_{10}O_5$. From the photosynthesis reaction (Eq. 2.1) and the glucose-cellulose reaction (Eq. 2.2) simplified to:

$$6CO_2 + 6H_2O + \text{Light} = C_6H_{12}O_6 + 6O_2 \quad (2.1)$$

$$C_6H_{12}O_6 = C_6H_{10}O_5 + H_2O \quad (2.2)$$

The oxygen in glucose, and therefore in cellulose, is derived solely from water taken up by the roots, as is the hydrogen. Any oxygen derived from CO_2 is expelled by the tree as O_2.

The primary source of water for trees is soil water; thus, the primary source of oxygen and hydrogen isotopes is also soil water and therefore much of the isotopic signal should reflect the isotopic signature of precipitation. There are several potential opportunities for fractionation before these isotopes become fixed in cellulose. The first fractionation occurs in the soil where evaporation can alter the original isotopic value. The depth at which the roots access the water can also effect the isotope value due to

differing isotopic values of groundwater for example is the water old or new or is it from winter or spring precipitation (McCarroll and Loader, 2004).

Once a tree sequesters water, no fractionation occurs until the water reaches the leaves, where transpiration preferentially removes the common isotopes (^{16}O and ^{1}H) from the tree reservoir, increasing $\delta^{18}O$ and δD values (Fig. 2.1.1). During glucose fixation, $\delta^{18}O$ increases by 27‰ for conifers (Roden *et al*., 2000), from the $\delta^{18}O$ value of the leaf water. When tree-ring cellulose is formed, from glucose, there is some exchange between glucose oxygen and xylem water in the trunk. The possible exchange of glucose oxygen with xylem water may be as high as 20% of the oxygen exchanging during the synthesis of cellulose from glucose via triose-phosphate (Roden *et al.*, 2000), dampening the signal imparted from evaporation in the leaves. This exchange of oxygens would imply that tree-ring $\delta^{18}O$ values will have a time lag component in the signal between glucose formation and cellulose formation, and thus is not a direct measure of the isotopic value of source water from a given time. Evaporation increases the $\delta^{18}O$ values of leaf water, therefore, $\delta^{18}O$ values of the glucose are higher than the $\delta^{18}O$ values of the original xylem water, and consequently the $\delta^{18}O$ values of the cellulose will also be higher. Evaporation will depend on several factors such as stomatal conductance and vapour pressure, both of which are linked to relative humidity (RH). Thus, the dominant environmental signals recorded in the $\delta^{18}O$ record of tree-rings are the isotopic value of the source water and the summer humidity.

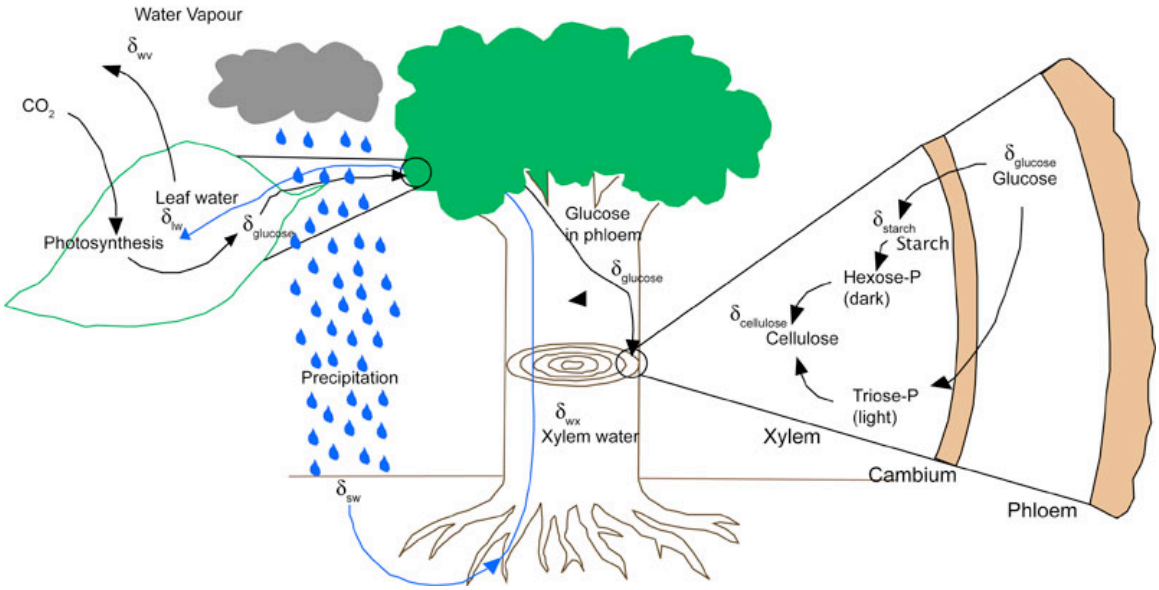

Figure 2.1.1: Schematic representation of the fractionation events undergone by oxygen and hydrogen before incorporation into tree-ring cellulose. δ_{sw} is the isotope value (H or O) of the source water, usually precipitation, δ_{wv} is the isotope value of water vapour, δ_{xw} is the xylem water isotope value, δ_{lw} is the isotope value of the leaf water, $\delta_{glucose}$ is the isotope value of the glucose, δ_{starch} is the isotope value of the starch and $\delta_{cellulose}$ is the isotope value of the cellulose. Arrows indicate the routes taken by water isotopes (H and O) from source water to final incorporation in cellulose (adapted from Roden *et al*., 2000).

Oxygen is not the only element in cellulose derived from water. Hydrogen in cellulose is also derived from water and its isotopic ratio is governed by many of the same processes affecting oxygen isotopes. Oxygen and hydrogen isotope fractionation factors in the leaf differ, but the processes causing fractionation (i.e. evaporation) are the same. During photosynthesis there is a marked discrimination against D (deuterium, ^{2}H). Therefore, glucose formed in the leaf is has a lower δD value than leaf water. The magnitude of this discrimination is uncertain and estimates have ranged from -100‰ to -171‰. When glucose is converted to cellulose, there is a similarly large fractionation in the opposite direction of 141‰ to 166‰ (Terwilliger *et al*., 1995; Roden *et al*., 2000; McCarroll and Loader, 2004). As with oxygen, exchange with xylem water increases δD values towards those of the source water. Roden *et al*., (2000) estimated that the degree of exchange is dependent on whether the conversion of sucrose to cellulose is via the hexose phosphate pathway or the triose phosphate pathway which depends on whether the glucose was broken down heterotrophicaly (during dark respiration) or autotrophicaly (during light photosynthesis). However, it may be more likely that the differing fractionation is related to whether the cellulose was formed directly from glucose or from starch. During the day a tree produces more glucose than it uses. Some of this glucose is converted directly to cellulose, corresponding to the autotrophic mechanism of Roden *et al*. (2000). The remaining glucose is converted to starch for the plant to use later. Plants break down this starch in the dark to access the stored glucose, some of which is used to form cellulose. This conversion of starch to cellulose would correspond to the heterotrophic mechanism mentioned by Roden *et al*. (2000). Hydrogen, due to the larger changes involved, is more

strongly influenced by RH than oxygen (Waterhouse *et al*, 2002), but like oxygen δD values reflect the isotopic values of precipitation.

2.2 Carbon Isotopes

Trees obtain their carbon during photosynthesis from CO_2 in the atmosphere. CO_2 enters the stomata of a trees leaves, which can be constricted by guard cells to control water loss. Thus, carbon gain and water loss are intimately related. Two main mechanisms of fractionation occur during the transition from atmospheric CO_2 to leaf carbon,. The first occurs when air diffuses into the stomata as CO_2 molecules consisting of ^{12}C will diffuse into the leaf more easily than the CO_2 composed of ^{13}C due to the size difference of the molecules. This size difference results in a fractionation due to diffusion of -4.4‰ (Leavitt and Long, 1991; McCarroll and Loader, 2004). The second fractionation occurs during photosynthesis, because biological processes prefer to use ^{12}C, resulting in a fractionation during carboxylation of about -27‰. The dominant environmental signals recorded in tree-ring $\delta^{13}C$ are stomatal conductance, which is related to RH, and the rate of photosynthesis (Fig. 2.2.1).

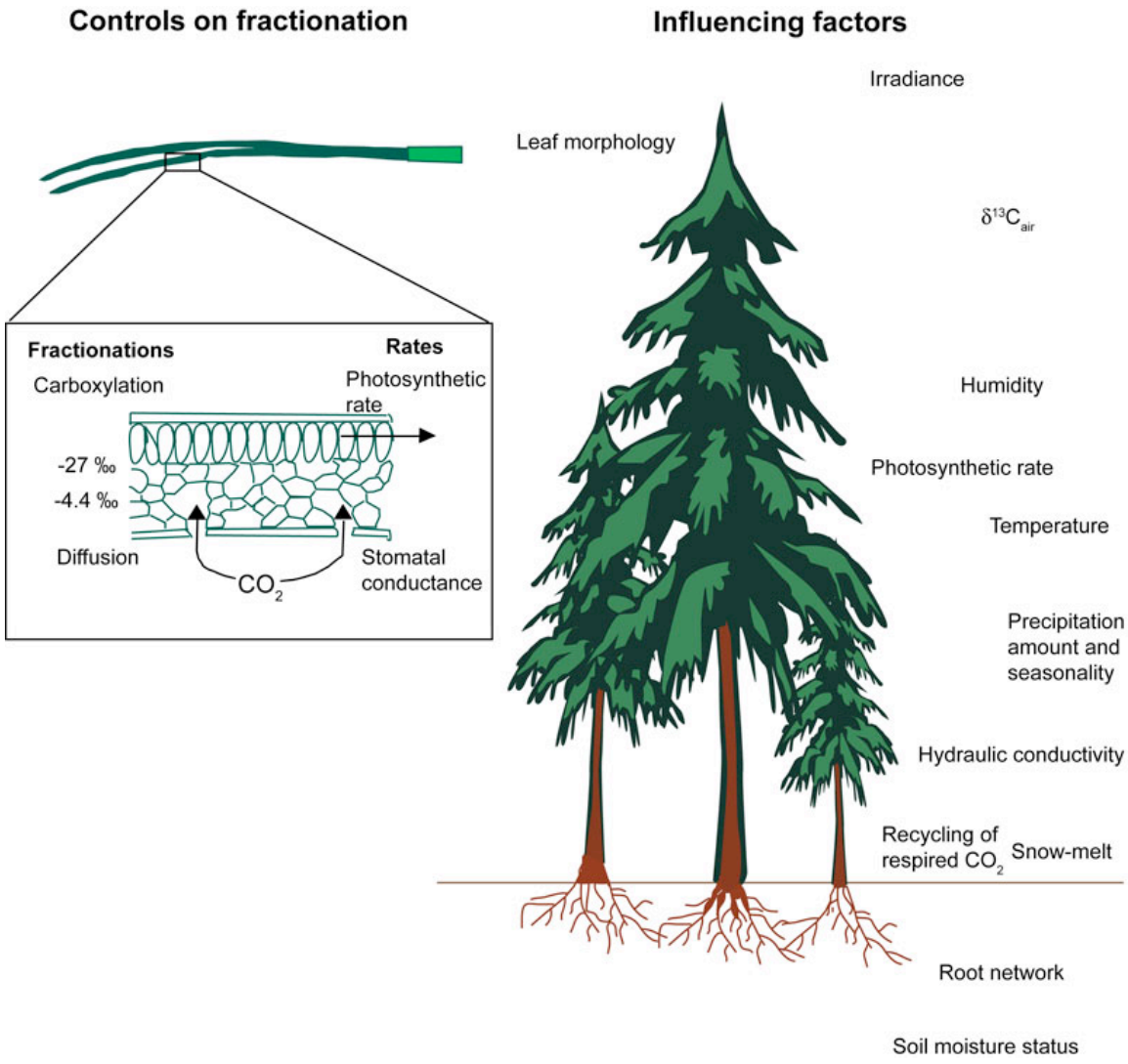

Figure 2.2.1: Schematic representation of the fractionation processes and controls on fractionation of carbon isotopes in a tree. Listed beside the trees are the factors that influence the $\delta^{13}C$ values of tree rings. In the box is a schematic of the inside of a leaf with the two primary fractionations, diffusion and carboxylation, listed on the left and the two rates that control $\delta^{13}C$ ratios listed on the right (adapted from McCarroll and Loader, 2004).

2.3 Technical background

Wood is a complex compound containing cellulose, hemi-cellulose, lignin, resins, tannins and other organic compounds (Barbour *et al.*, 2002). Wilson and Grinsted (1977) discovered that different components of wood have different isotopic values related to differing fractionation processes. These components confound the determination of climate signals from bulk, mixed-component samples. The confounding signals led researchers to focus on α-cellulose, which is the dominant component (~44 wt. %) and one of the easiest to isolate from wood. To analyze wood for $^{18}O/^{16}O$, $^{13}C/^{12}C$, and D/H values, it is first necessary to isolate the α-cellulose component of the wood. This analytical technique addresses several important issues including heterogeneity of the samples, reduction of diagenetically induced differences in other phases, such as lignin, and linking the component studied to the framework of the tree-ring (since cellulose forms the cell walls of the trachieds) and the isotopic values to a particular growth phase (McCarroll and Loader, 2004).

δD analyses require conversion of α–cellulose to cellulose nitrate. The reason for this is due to a high degree of exchangeability of hydrogen in the cellulose with other sources of hydrogen, such as atmospheric water or chemicals during processing. It is thus necessary to eliminate the exchangeable hydrogen via nitration of the cellulose. The exchangeable hydrogens are located in the hydroxyl component of cellulose, and nitration replaces the hydroxyl group with a nitrate group, thereby eliminating the hydroxyl-bonded hydrogen from the cellulose. This process precludes the use of nitrated cellulose for oxygen isotope analyses, therefore un-nitrated α-cellulose must be used for $\delta^{18}O$ studies.

3. Materials and Methods

3.1 Geological Setting

The site studied is located in Central Ellesmere Island near the head of Strathcona Fiord (Fig 3.1.1). Stratigraphicaly the site lies within the Beaufort Formation, a predominantly fluvial unit that forms part of the Sverdrup Basin (Fig. 3.1.2) (Fyles, 1989). Numerous outcrops of the Beaufort formation exist throughout the Sverdrup Basin, many of them containing fossil plant material (Matthews and Ovenden, 1990; Elias and Matthews, 1997). Some units have been interpreted as marine units based on fossil evidence, while other facies include prodelta and delta sequences (Fyles *et al*., 1998). No unequivocal Pliocene marine units exist in the study area, indicating an entirely non-marine depositional setting.

The Strathcona section at N 78° 29.271′ W 82° 37.973′ consists of two primary facies. The first facies is composed of arkosic gravels with coarse sand, suggesting a fluvial depositional setting. Gravel clasts comprised predominantly of chert and were most likely derived from the underlying Cretaceous units. The second facies consists of fine-to-medium grained sand with intercalated silt and discontinuous peat layers. The sand is cross-bedded in the coarser layers and planer bedded in the finer layers; both layers contain abundant plant macrofossils (Fig. 3.1.3). These sand layers probably represent crevasse splay deposits, with the macroflora becoming trapped in the sands during flooding. The peat layers associated with the sands suggest this was a peat mire/alluvial floodplain environment. Facies indicate that the depositional environment was a braided river system. The gravel units probably represent alluvial wash from the surrounding uplands into the braided river valley or possibly gravel bars at the river

bends. Coeval units from Prince Patrick Island and Ellesmere Island have also been interpreted as braided fluvial deposits (Fyles, 1989; Fyles, 1990; Matthews *et al*., 1990). Younger units on Meighen Island have marine units underlying fluvial sand and peat and they have been interpreted as a fluvio-deltaic environment (Fyles *et al*., 1991). Since Meighen Island is the only Beaufort site with marine sediments and is also the most northerly site, it is possible that the Beaufort Rivers were flowing north, towards the palaeoshoreline.

Hulbert and Harington (1999) and Tedford and Harington (2003) described a rich mammal fauna from a nearby, likely correlative, site providing biostratigraphic control, placing our tree in the Early Pliocene (4-5 million years old). The tree is associated with a diverse flora typical of northern taiga, including spruce (*Picea*), dwarf birch (*Betula*), larch (*Larix*) and several mosses (Hulbert and Harington, 1999).

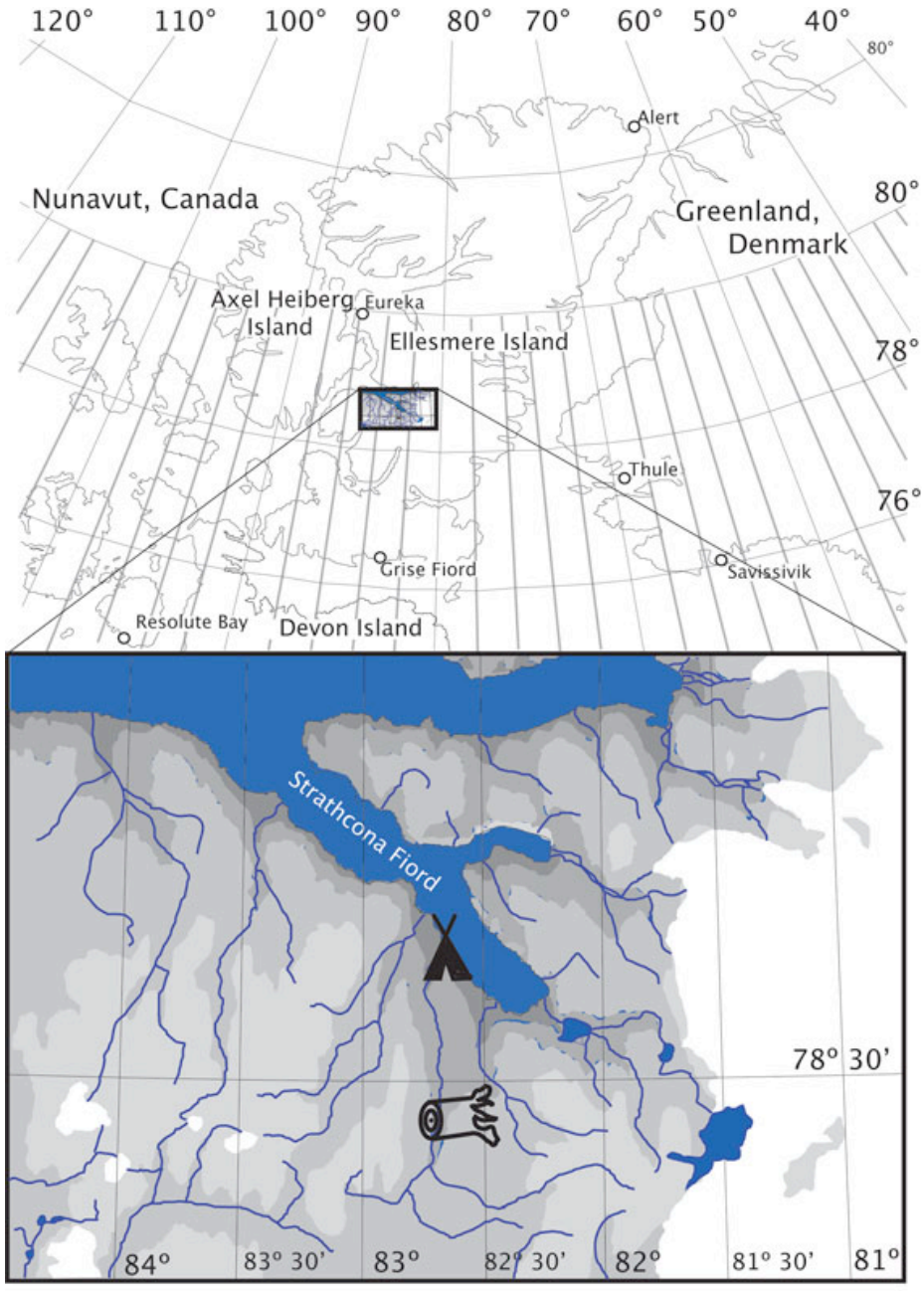

Figure 3.1.1: Map showing Strathcona Fiord in central Ellesmere Island the site where Pliocene wood was collected. Base camp is indicated by the tent, the log indicates site where the trunk was collected. Shading represents elevation a 100 m contour interval.

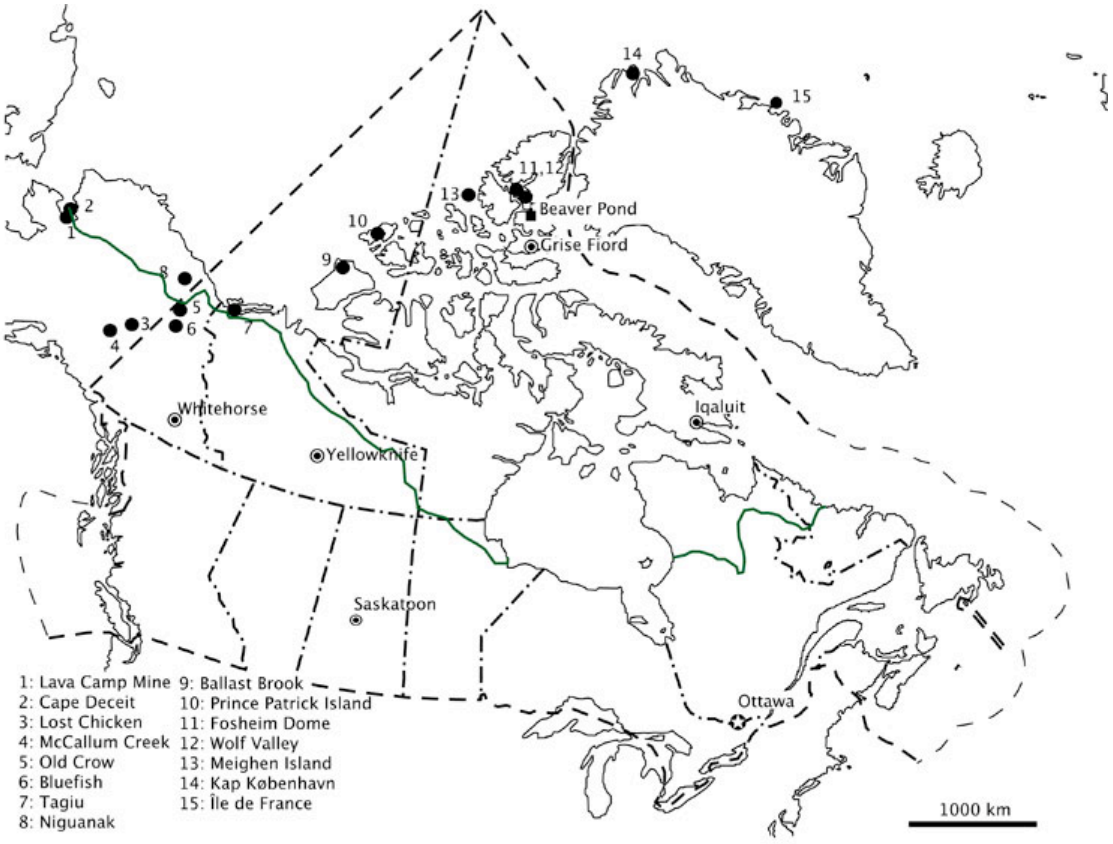

Fig. 3.1.2: Map shows distribution of Pliocene Beaufort Formation fossil sites in the North American Arctic. Illustration includes the extent of the present northern tree-line (adapted from Elias and Matthews, 1997).

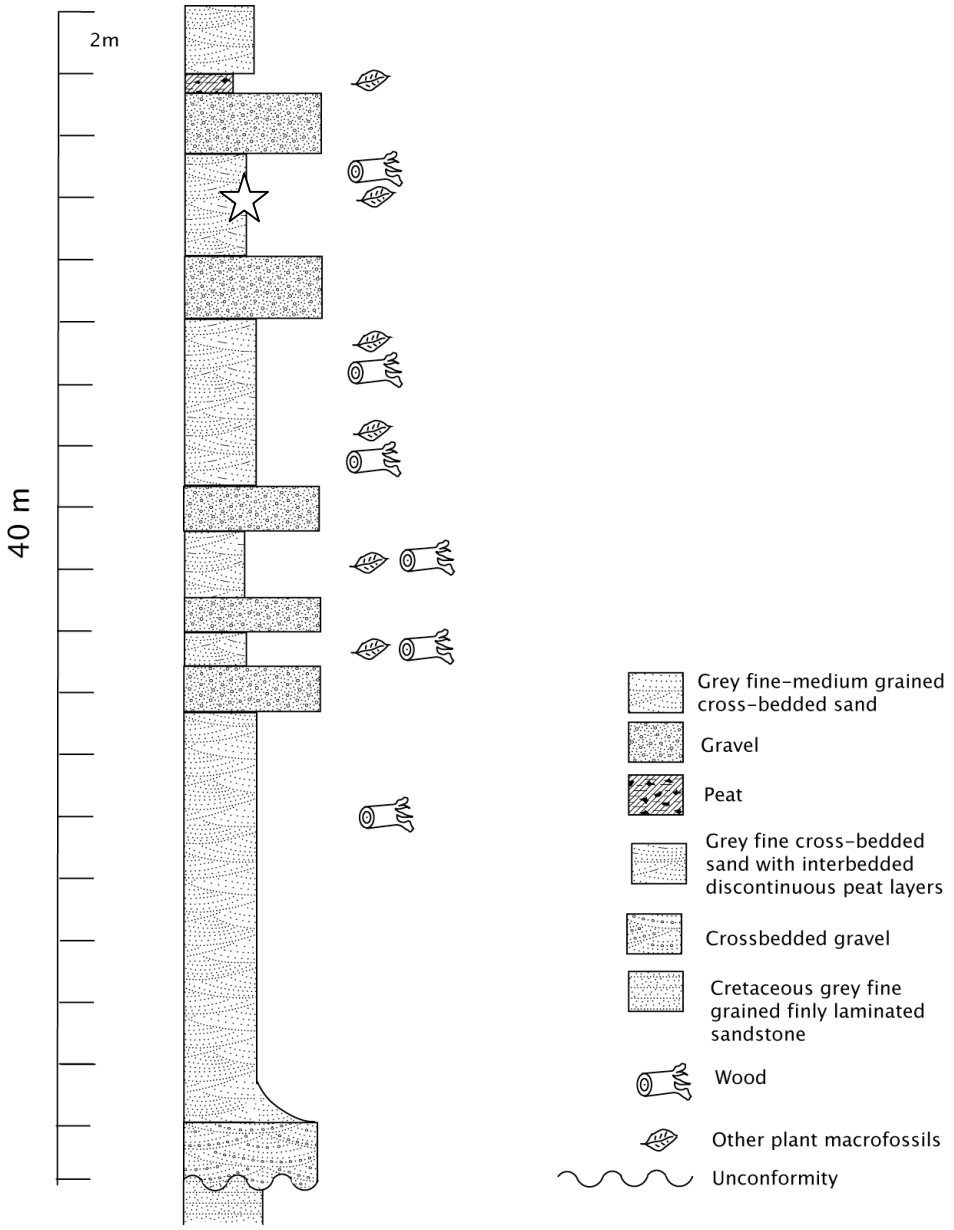

Fig. 3.1.3: Stratigraphic column of the Strathcona Fiord site of the Beaufort formation. Column shows all fossil bearing units, indicated by logs where wood was present and leaves where other plant material was present. The star indicates the level from which the sample analyzed in this study was taken.

3.2 Sampling procedure and analysis

Fossil wood from a single trunk was sampled by first slicing a transverse disk using a Japanese Ryoba 330 fine toothed saw. The wood was sliced into rectangular blocks and then individual rings were sampled using a scalpel to shave off thin slices of ~50 μm in width, in the laboratory. The narrow yearly ring widths (in some cases as thin as 0.1 mm), made it difficult to separate early wood from late wood. However, whenever rings were thicker than 0.5 mm, early wood was sampled separately from late wood.

The method outlined by Loader *et al*. (1997) was used to isolate the α-cellulose component of the sampled rings of the wood. Samples were placed in soxlet thimbles and immersed in a 2:1 solution of toluene and methanol for 4 hours to remove resins. Samples were rinsed once in Acetone and subsequently rinsed 3 times in distilled water. Ten mL of a solution consisting of 1 L deionized water, 15 g of sodium chlorite and 10 mL of acetic acid was added to each sample, with another 10 mL of solution added every 4 hours during the 48 hour period of sonication. Samples were moved to an ultrasonic bath at 70º C for 2 days until lignin was completely removed indicated by the samples turning completely white. Deionized water heated to 70º C was used to rinse the samples followed by a rinse in 20º C deionized water. Ten mL of 10% sodium hydroxide was added to the samples that were subsequently placed in an ultrasonic bath at 80º C for 2 hours, samples were removed from the ultrasonic bath and rinsed with deionized water. Ten mL of 17% sodium hydroxide was then added to the samples and they were placed in an ultrasonic bath at 20º C for 2 hours. This step ensures removal of all sugars and

hemicellulose from the samples. The samples were rinsed in deionized water one final time and placed in a vacuum oven at 40° C to dry for 12 hours.

δD analyses require conversion from α–cellulose to cellulose nitrate. For the nitration step, the acetic anhydride method outlined by Sternberg (1989) was used. Acetic anhydride (450 mL) was added to 269 mL of fuming nitric acid (90% nitric acid) in a mixing flask set on a magnetic stir plate and was stirred constantly. This reaction is highly volatile and must be kept cool. To this end the flask was placed in a plastic container containing a mixture of 50% ethylene glycol and water to which enough liquid nitrogen was added to keep the reaction at ~ -20° C. The nitration solution was added to 50 mL centrifuge tubes containing α-cellulose samples and placed in ice to be kept at 4° C for 4 hours. The impure cellulose nitrate was then dissolved in acetone, thereby isolating it from incompletely nitrated cellulose. Samples were then centrifuged and the supernatant, containing the dissolved cellulose nitrate, separated and left in a 25 mL beaker in the fume hood until the solution thickens. The solution is then squirted vigorously with water resulting in precipitation of the purified cellulose nitrate. Samples are then freeze dried for analysis.

δD and $\delta^{18}O$ values were determined at the Saskatchewan Isotope Laboratory using a Thermo Finnigan TC/EA coupled to a Thermo Finnigan Delta Plus XL mass spectrometer in continuous flow mode via a Conflo III interface. $\delta^{13}C$ values of cellulose were determined using a Thermo Finnigan Flash EA via oxidation directly coupled to a Thermo Finnigan Delta Plus XL mass spectrometer via a Conflo III.

Several gastropods were isolated from peat samples located stratigraphicaly above the layer, indicated by a star in figure 3.1.3, containing log US 814. These gastropod

shells were crushed and analyzed for $\delta^{18}O_{aragonite}$ on a Kiel carbonate device coupled to a Thermo Finnigan 253 mass spectrometer in continuous flow mode.

Figure 3.2.1: Photograph of the specimen US 814. Evident in the photo is the excellent preservation of the specimen and the stunted twisted growth of the specimen.

3.3 Data analysis

3.3.1 Mathematical modeling

Edwards *et al*. (2000) examined the relationship between RH and $\delta^{13}C$ and developed a model relating the two via the following equation.

$$RH = (\delta^{13}C_{cellulose} + 6) - (- 0.15 * T) / - 0.17 \qquad (3.1)$$

When our $\delta^{13}C$ data is examined using this equation, an average humidity for the site of 81 % is calculated. As seen in Edwards *et al.* (2000) modeled values from this equation appear to be highly locally dependent and in the absence of other information there is no way of knowing how accurate our modeled humidity was.

In an effort to understand the relationship between tree-ring isotopes and their environment, Roden *et al.* (2000) developed mathematical models to determine factors (i.e humidity, temperature, physiology) that influence isotope ratios. Trees were grown

under controlled laboratory conditions and were subsequently analyzed for $\delta^{18}O$ and δD values. Their premise is that oxygen and hydrogen isotopes are incorporated into cellulose from leaf water after several fractionation processes during the transition (Eq 3.2 and 3.3). Where f_o and f_H is the fraction of carbon bound oxygen and hydrogen, respectively. $\delta^{18}O_{wx}$ and δD_{wx} are oxygen and hydrogen isotope ratios of xylem water, ε_o is the biological fractionation factor for oxygen in sugar converting to cellulose, ε_{HH} is the biological fractionation factor for hydrogen in sugar converting to cellulose in a heterotrophic reaction, while ε_{HA} is the biological fractionation factor for hydrogen in sugar converting to cellulose in an autotrophic reaction. δD_{wl} and $\delta^{18}O_{wl}$ are the oxygen and hydrogen isotope ratios of the leaf water.

$$\delta^{18}O_{cellulose} = f_o * (\delta^{18}O_{wx} + \varepsilon_o) + (1 - f_o) * (\delta^{18}O_{wl} + \varepsilon_o) \quad (3.2)$$

$$\delta D_{cellulose} = f_H * (\delta D_{wx} + \varepsilon_{HH}) + (1 - f_H) * (\delta D_{wl} + \varepsilon_{HA}) \quad (3.3)$$

Their model was subsequently field tested in a study of riparian vegetation and was able to explain almost all of the variance in both δD_{CN} and $\delta^{18}O_{cellulose}$ values (Roden and Ehleringer, 2000). Subsequently Waterhouse *et al*. (2002) conducted a test of the existing Roden *et al.* (2000) model using Oak (*Quercus*) tree-ring isotopes in central England and discovered that although the model explained all of the variance in the oxygen isotopes it was not able to explain the variance in hydrogen isotope values. The Roden *et al.* (2000) model relys on knowledge of modern plant physiology, leaf water and xylem water isotope ratios rendering it useless in a palaeoclimate context, due to a lack of knowledge of these factors. Another model devised by Anderson *et al.* (2002) is slightly more useful for palaeoclimatology because it is has fewer unknowns (Eq. 3.4).

$$\delta^{18}O_{sw} \approx \delta^{18}O_{cellulose} - (1 - f)(1 - h)(\varepsilon_e + \varepsilon_k) - \varepsilon_{biochem} \quad (3.4)$$

Where $\delta^{18}O_{sw}$ is the oxygen isotope value of source water, *f* is the fraction of leaf water not subject to evaporation and accounts for the alteration of the isotope value of photosynthate due to stem water interaction. ε_e is the liquid-vapor equilibrium fractionation factor (Manjoube, 1971), ε_k is the liquid-vapor kinetic fractionation, dependent on airflow dynamics at the leaf boundary layer, *h* is relative humidity and $\varepsilon_{biochem}$ is the biologic fractionation factor for sugar converting to cellulose calculated as 27 ± 3‰. ε_k varies depending on species; however, for conifers it has been inferred to be 28‰ (Anderson *et al*., 2002). Anderson *et al*. 2002 also found that a variable *f* value, dependent on humidity, was much more valuable in the model than a fixed value for *f*. Use of the Anderson *et al.* (2002) model requires knowledge of humidity, temperature (to calculate ε_e) and/or source water value.

3.3.2 Wavelet analysis

Continuous transform wavelet analysis is a technique, first developed for use in signal processing, but has since been used in a variety of applications, including earth, environmental and atmospheric sciences (Grindsted *et al.* 2004; Torrence and Compo, 1998). Unlike Fourier transform analysis, continuous transform wavelet analysis identifies both frequency and duration of occurrence of cyclicity in a time-series record. One can also identify changes in frequency with time, as is seen in parts of the Pliocene record. The wavelet analysis techniques used here are minor modifications of the Matlab routines provided by Torrence and Compo (1998) and Grinstead *et al*. (2004). A Morlet wavelet was used because it provides the best localization of information in both the time and frequency dimensions. A test data set comprising a signal made up of several

independent or smoothly varying known periodicities has been used to illustrate the capabilities of continuous wavelet transform analysis (Fig. 3.3.1). The signal is a combination of different sine waves (each with a 40 year period but with different amplitudes and means); a signal with an 80-year period; one instantaneous, large spike; and a signal with period smoothly varying from 80 to 20 years. The wavelet spectrum clearly identifies intervals in which individual signals are present or absent. Note the abrupt shifts to different periodicity where breaks occur in the signal and the smoothly varying change in high power associated with the 80 to 20 year change in period of the input signal. Note also, that a change in amplitude for a signal of constant period does not influence the identification of the periodicity.

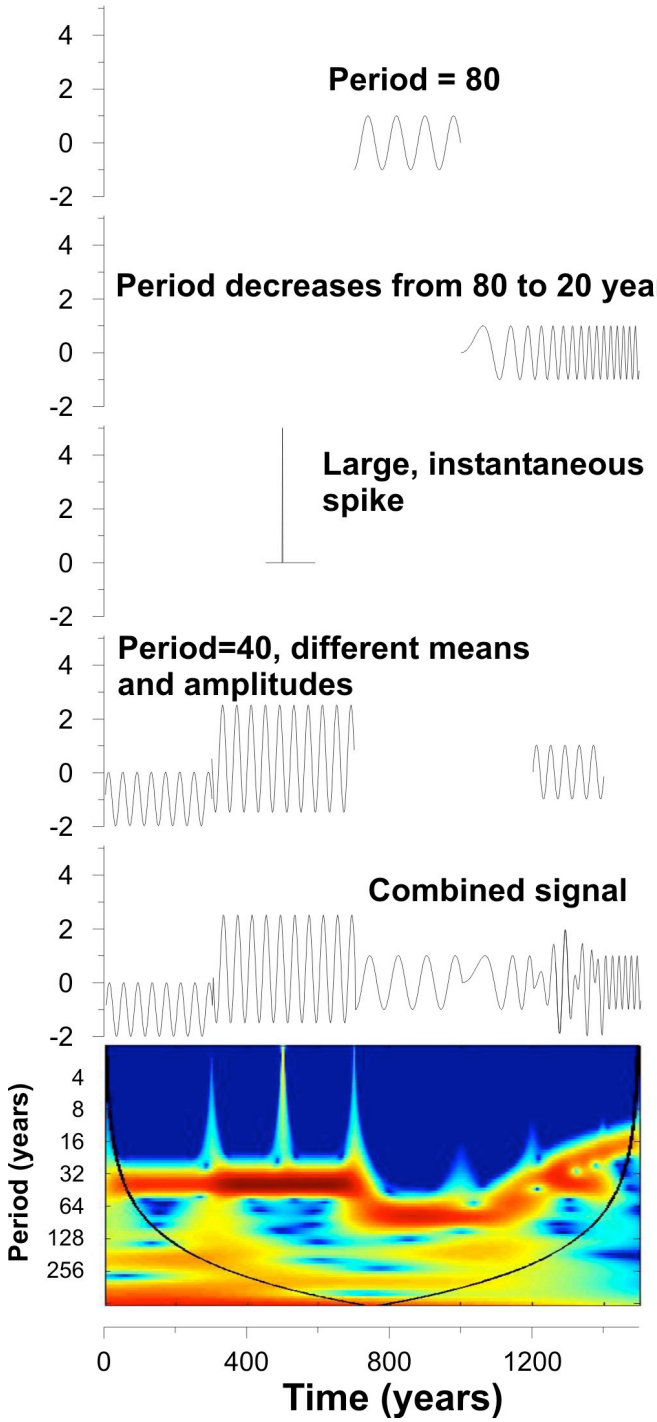

Figure 3.3.1: Test data set illustrating the capabilities of the wavelet analysis used in our study, high power in the wavelet spectrum derived from this signal is indicated by red colours and low power by blues. (figure courtesy of B. Eglington).

4. Results

4.1 Wood anatomy and tree growth

Most conifer wood consists of tracheids, vertically arranged and lignified cells. Tracheids conduct water and nutrients from the roots through the tree and provide support. Tracheids of early wood (wood formed in the spring and early summer in temperate climates) often have relatively large diameter with thin cell walls. As trachieds form radialy they retain their tangential size and form fairly regular files of cells. Towards the end of growth, tracheids are smaller with thick cell walls and often have a flattened appearance; this is known as latewood (wood formed in the fall in temperate climates) (Jane, 1970).

To identify wood specimens, wood anatomy must be viewed from three perspectives. The transverse direction (TS), is horizontally through the trunk and illustrates features such as growth rings. Radial sections (RLS) run vertically through the centre of the trunk and tangential (TLS) also vertical but cut along the edge of the trunk. Blocks of wood were cut and mounted on a stage and gold coated for viewing in a scanning electron microscope. In RLS tracheids exhibit uniseriate (45%), biseriate (54%) or triseriate (1%) bordered pitting. Pits are circular and have a diameter of 10 μm; pits are almost always (98%) touching in early wood or spaced 1 μm apart (2%) in late wood. Multiseriate pits are oppositely arranged (100%). Rays are 1.35 to 1.76 mm long and have thick walled cells 70 μm, 5 μm wide and 7 μm high. Cross-field pitting is pinoid and piceoid consiting of 1-2 alternately arranged, where more than one, circular pits. In TLS trachied walls are blank (do not contain bordered pits) and rays are uniseriate or

fusiform (containing horizontal resin ducts (20%). Torsion checks are present on some trachied walls in TLS. Rays are 2-12 cells high, spaced about 12 rays/linear mm. Fusiform rays contained horizontal resin ducts, 41-45 μm by 38-44 μm in diameter. Axial resin ducts 52-56 by 55-59 μm are present in TS ringed by 8-10 epithelial cells with cell widths of ~15 μm. Axial resin ducts are concentrated in the latewood and most often occur as two adjoining ducts. The wood has been identified through these wood anatomical characteristics as belonging to the *Larix* genus (Fig. 4.1.1) (Greguss, 1955). *Larix* cones and leaves are quite common in the associated peat deposits, therefore, it is reasonable to conclude that this specimen is indeed *Larix*.

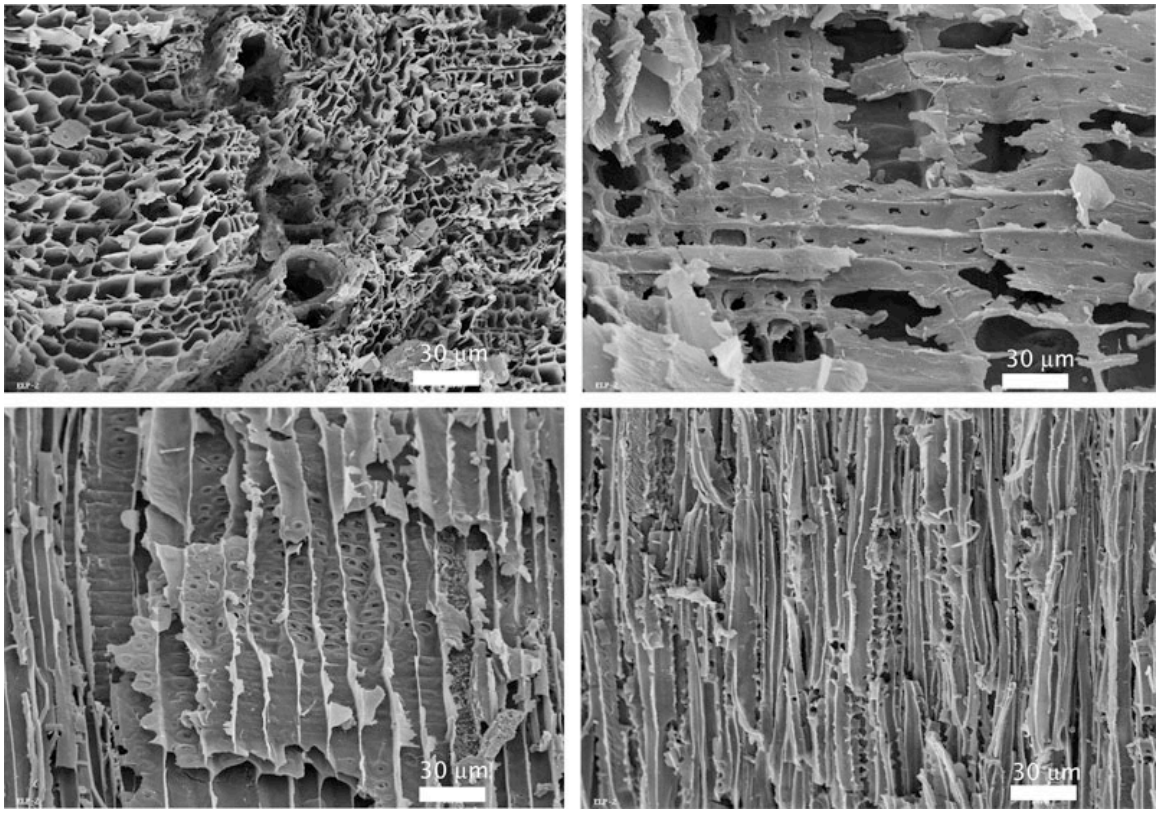

Figure 4.1.1: A) Example of a traumatic ring (frost ring) present in TS of wood specimen ELP-001. **B)** RLS section of wood showing bordered pitting, note the high percentage of biseriate trachieds. **C)** RLS section showing cross-field pitting. **D)** TLS section showing rays note the lack of many biseriate rays and the presence of torsion checks in the upper left corner of the image.

4.2 Tree-ring widths

The Pliocene log, approximately 22 cm wide and 1.72 m tall from roots to flared upper branches, has the narrow rings, stunted development, and curtailed vertical growth characteristic of northern and alpine tree-line vegetation. Growth rings were narrow rings (mean = 0.34 mm max = 1.5 mm n=203), comparable to ring widths of modern *Larix* from approximately 72° N in Siberia (Creber and Chaloner 1985). Tree-ring widths for 203 consecutive years of the Early Pliocene are shown in Figure 3.2.1. Ring widths vary from 1.5 to 0.05 mm with a mean of 0.34 mm. A sharp reduction in ring width at year 80 is likely due to tree maturity, increasing stand density, availability of nutrients, insect predation and several other factors (Creber, 1977). Periods of wide ring widths occurred at years 28-35, 59-76, 106 -112 and 131-154, periods with narrow rings, exist at years 18-26, 51-58, 100-104, 155-161 and 186-191. In Boreal Forests temperature is inferred to be the dominant factor affecting tree growth (Briffa, 2000). Thus, narrow ring widths may represent cold periods while wide rings likely formed during warm periods. A temperature interpretation of ring widths is not entirely satisfactory because there are many other factors such as availability of water, nutrient availability, irradiance, insect predation, and the length of the growing season that may also affect tree growth (Creber, 1977). A multi-proxy study permits evaluation of these growth factors. Each proxy studied is affected by different environmental factors in unique ways and these differences can be used to isolate the actual environmental factors affecting the tree.

Mean sensitivity is a measure of the average year-to-year variability in growth rings (Creber and Francis, 1999). Uniform ring width suggests consistent conditions and

has mean sensitivity values below 0.3. Conversely highly variable widths would indicate variable growing conditions (termed sensitive) and would have values above 0.3. The Pliocene log has a mean sensitivity value of 0.35 placing this tree in the sensitive range indicating that highly variable conditions were common for this tree. False rings form when growth is interrupted by a myriad of factors such as drought in the summer or an early autumn or late spring cold period. Frost rings form if, during growth, ice crystals form inside the vascular cambium and damage the growth layer (Glerum and Farrar, 1966). As temperatures rise, the vascular cambium grows only at undamaged parts of the Cambium. Therefore larger than normal cells are produced to fill the gaps created by the damaged tissue (Fig. 4.1.1A). Six frost rings were observed in the wood indicating that early, or late, cold periods were common in this forest.

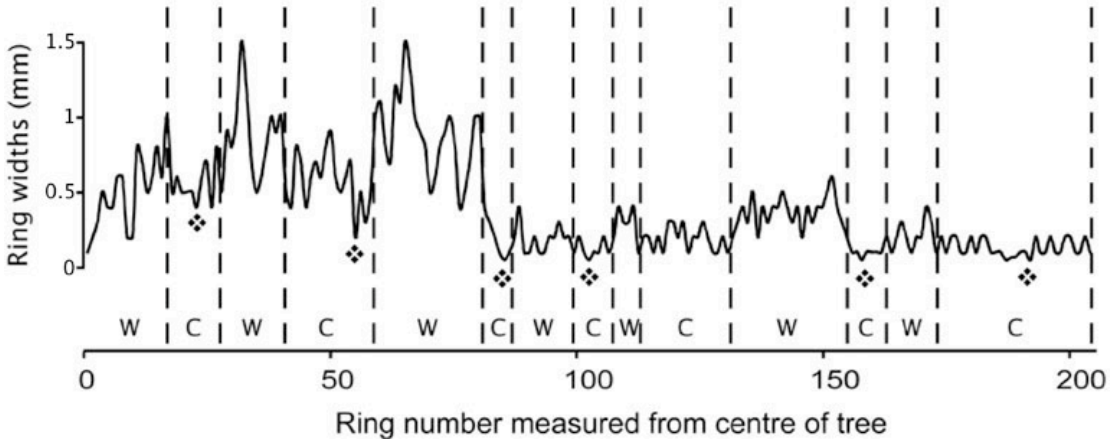

Figure 4.2.1: Ring width record for the Pliocene log measurements start with 0 as the centre of the tree and measure out to 203. W = warm periods, C = cold periods and ❖ = frost rings. Warm and cold periods are discussed in section 5.1.

4.3 Stable isotopes in wood

Figure 4.3.1 presents $\delta^{13}C_{cellulose}$ values for 203 consecutive years of the Early Pliocene, $\delta^{13}C_{cellulose}$ values range from –23.9 ‰ to –20.2 ‰ VPDB and reveal several prominent peaks (years 12-18, 40-51, 57-68, 138-159 and 174-196) and prominent troughs (years 18-25, 29-40, 51-55, 70-74, 160-173 and 198-203). Also evident in the record is a period of lower variability between years 93-137.

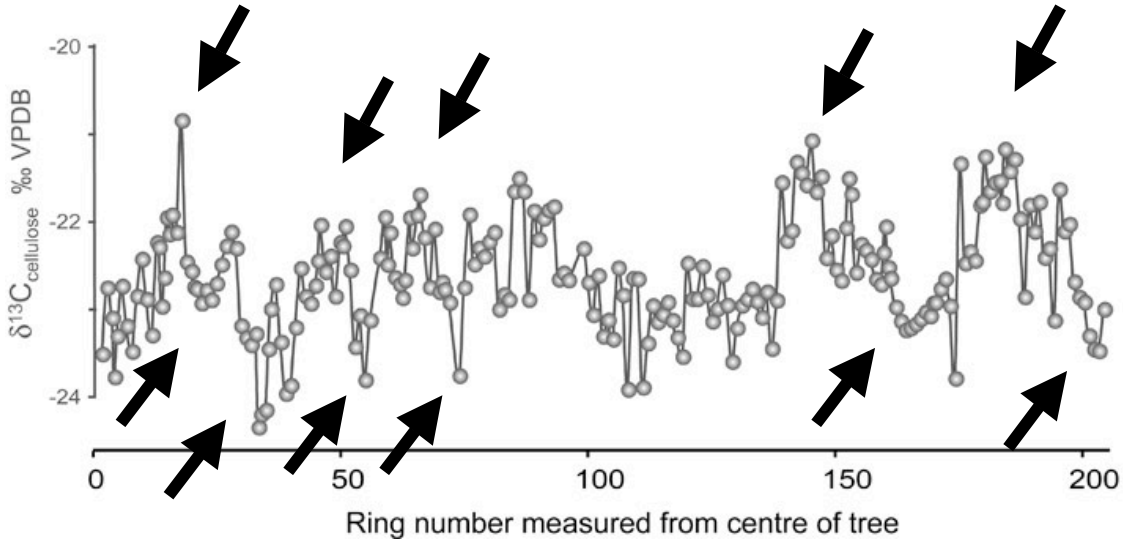

Figure 4.3.1: $\delta^{13}C_{cellulose}$ isotope record from Pliocene wood. Rings are numbered consecutively out from the centre of the tree.

$\delta^{18}O_{cellulose}$ values for the Early Pliocene, presented in Figure 4.3.2, range from 15.4 ‰ to 24.5 ‰ VSMOW. $\delta^{18}O_{cellulose}$ values were high in years 10-18, 24-30, 73-77, 137-155, 183-187 and 193-200, and low during years 19-23, 37-40, 155-165 and 173-182. The $\delta^{18}O_{cellulose}$ record, like the $\delta^{13}C_{cellulose}$ record, also showed a period of low variability from year 105 to 137.

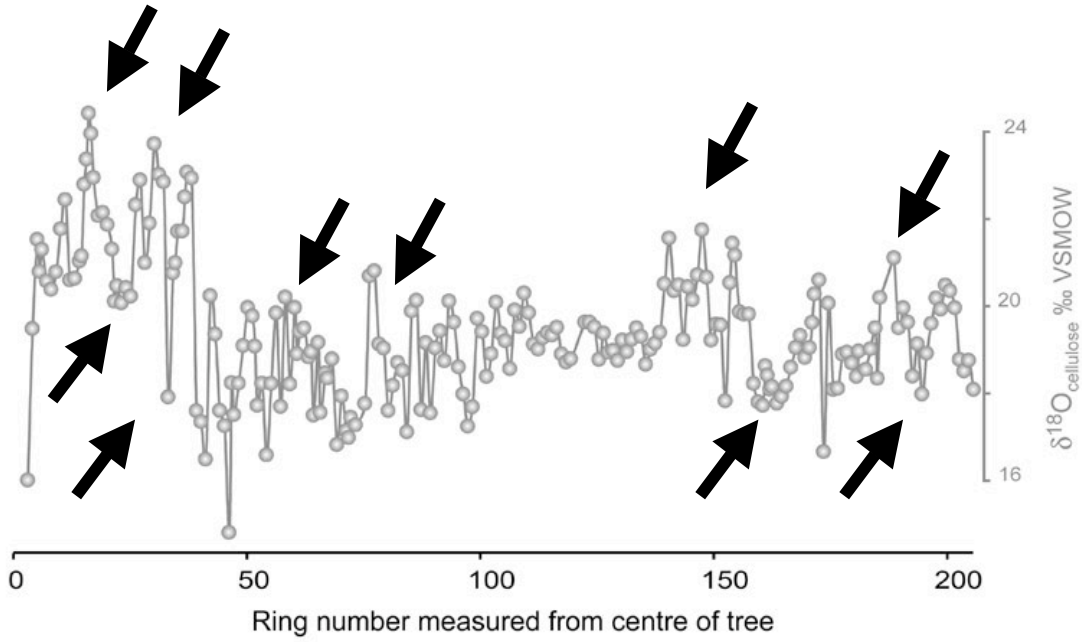

Figure 4.3.2: $\delta^{18}O_{cellulose}$ record for Pliocene wood. Rings are numbered from the centre of the tree outwards towards the edge.

$\delta D_{cellulose\text{-}nitrate\ (CN)}$ values for the Early Pliocene ranging from –204 ‰ to –157 ‰ VSMOW are presented in figure 4.3.3. Beginning at year 80 δD values decreased from –170 to –204 ‰ VSMOW coinciding with a decrease in ring widths. However, δD values increased after year 98 to values averaging around –180 ‰ VSMOW while ring widths remain narrow. Decreased variability was observed between years 95 and 137.

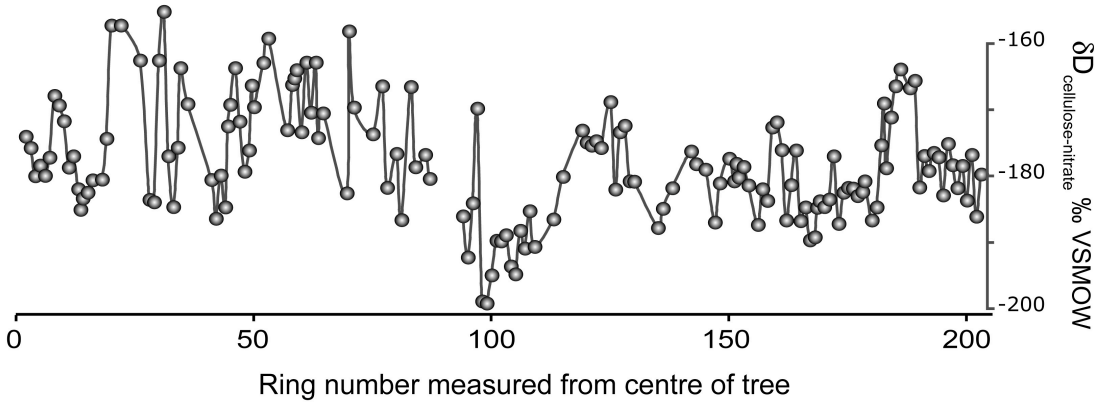

Figure 4.3.3: δD_{CN} values for 203 years of the Early Pliocene. Rings are numbered from centre of the tree outward.

4.4 Palaeoenvironmental modeling

Using the mathematical modeling equations of Roden *et al.* (2000) and Anderson *et al.* (2002) we were able to obtain some estimates of temperature and source water using the isotope values derived from the Pliocene log. To use these models we need to be able to infer or calculate values for temperature, humidity, and/or source water value. The palaeotemperature of the Pliocene site was calculated using $\delta^{18}O$ values derived from

fossil gastropods using the aragonite temperature equation of Patterson *et al.* (1993). The average gastropod growing season temperature was calculated as 14.4 ºC. Using modern relative humidity for sites in Northern Canada, Norway, Siberia and Alaska an average Boreal Forest humidity of 70 % was calculated. Source water for each year was then calculated using these parameters and the Anderson et al. (2002) equation. In order to get a lake water value to use in the calculation of palaeotemperature from the gastropods, several moss fragments were isolated from the peat, processed to α-cellulose and analyzed for $\delta^{18}O_{cellulose.}$ Since aquatic plants would not undergo evaporative fractionation, the $\delta^{18}O_{cellulose}$ value should be equal to the $\delta^{18}O_{water}$ value, minus the 27‰ biological fractionation factor. The source water value calculated from the $\delta^{18}O_{cellulose}$ value of tree rings (–18.3 ‰ VSMOW) is similar to that calculated from the peat (–21.2 ‰ VSMOW; table 4.4.1). It is possible that the peat values are more negative because peat would more closely reflect ground water while tree-ring values may reflect greater evaporative enrichment. Although the individual annual values calculated using the Anderson *et al*., (2002) equation, do not appear real (values range from –106 to 284° C), the average temperature works out to 11° C. Using the Roden *et al*. (2000) equation with inferred values for leaf water ($\delta^{18}O_{cellulose}$ – 27‰) and the same *f* and *h* values used for the Anderson *et al*., (2002) equation calculations, we were able to calculate annual source water values from the tree. Average $\delta^{18}O_{sw}$ values calculated with the Roden *et al*. (2000) equation were ($\delta^{18}O$ = –18.3 ‰) nearly identical to the average value calculated using the equation of Anderson *et al*., (2002).

Ring number	δ^{18}Osw (Anderson)	δ^{18}Oxw (Roden)	δDxw (Roden)	Temp. (Anderson)	Temp. (Roden)
1.0	-21.8	-21.8	-221.2		13.4
2.0	-18.3	-18.3	-221.2	-1.6	13.4
3.0	-16.2	-16.2	-223.1	-56.7	13.4
3.5	-16.9	-17.0	-225.4	-39.8	13.4
4.0	-16.4	-16.4	-227.7	-51.7	13.4
5.0	-17.2	-17.2	-226.0	-34.3	13.4
6.0	-17.3	-17.4	-227.6	-29.2	13.4
7.0	-16.9	-17.0	-224.7	-39.7	13.4
8.0	-15.9	-16.0	-214.5	-61.8	13.4
9.0	-15.3	-15.3	-216.1	-74.6	13.4
10.0	-17.1	-17.2	-218.7	-34.9	13.4
11.0	-17.1	-17.1	-226.3	-36.0	13.4
12.0	-16.7	-16.7	-224.4	-45.7	13.4
12.5	-16.6	-16.6	-197.6	-48.4	13.4
13.0	-14.9	-14.9	-229.8	-80.9	13.4
13.5	-14.3	-14.3	-233.2	-90.4	13.4
14.0	-13.2	-13.3	-231.3	-106.0	13.4
14.5	-13.7	-13.7	-230.9	-99.4	13.4
15.0	-14.7	-14.8	-230.4	-83.5	13.4
16.0	-15.6	-15.7	-228.4	-67.9	13.4
17.0	-15.6	-15.6	-228.3	-69.2	13.4
18.0	-15.8	-15.9	-228.3	-63.8	13.4
19.0	-16.4	-16.4	-221.6	-51.9	13.4
19.5	-17.6	-17.7	-212.3	-21.5	13.4
20.0	-17.3	-17.3	-203.0	-31.5	13.4
21.0	-17.7	-17.7	-203.0	-20.4	13.4
22.0	-17.3	-17.3	-203.0	-30.4	13.4
23.0	-17.5	-17.5	-204.5	-24.8	13.4
24.0	-15.4	-15.4	-205.9	-72.5	13.4
25.0	-14.8	-14.8	-207.3	-82.6	13.4
26.0	-16.7	-16.8	-208.8	-44.8	13.4
27.0	-15.8	-15.8	-220.1	-64.4	13.4
28.0	-14.0	-14.0	-231.5	-95.9	13.4
29.0	-14.7	-14.7	-232.0	-84.7	13.4
30.0	-14.8	-14.9	-208.8	-81.9	13.4
31.0	-19.9	-19.9	-200.8	72.5	13.4
32.0	-17.0	-17.0	-224.4	-39.1	13.4
32.5	-16.7	-16.8	-228.6	-44.7	13.4
33.0	-16.0	-16.0	-232.8	-60.6	13.4
34.0	-16.0	-16.0	-223.0	-60.8	13.4
34.5	-15.2	-15.2	-210.0	-75.8	13.4
35.0	-14.6	-14.6	-213.0	-85.6	13.4
36.0	-14.8	-14.8	-215.9	-83.4	13.4

37.0	-20.2	-20.2	-217.2	96.0	13.4
38.0	-20.4	-20.5	-218.4	118.5	13.4
39.0	-21.3	-21.3	-219.7	283.9	13.4
40.0	-17.5	-17.5	-220.3	-25.2	13.4
41.0	-18.4	-18.4	-221.0	2.8	13.4
42.0	-20.2	-20.2	-219.4	95.4	13.4
43.0	-20.5	-20.5	-228.3	128.1	13.4
44.0	-23.0	-23.0	-234.7		13.4
44.5	-19.5	-19.5	-227.6	52.7	13.4
45.0	-20.3	-20.3	-232.8	103.5	13.4
46.0	-19.5	-19.6	-219.6	53.1	13.4
47.0	-18.7	-18.7	-216.0	12.7	13.4
48.0	-17.8	-17.8	-210.0	-17.3	13.4
49.0	-18.0	-18.0	-218.7	-11.3	13.4
49.5	-18.7	-18.7	-227.0	13.2	13.4
50.0	-20.0	-20.1	-223.5	86.1	13.4
Averages	**-18.3**	**-18.3**	**-225.0**	**11.1**	**13.4**

Table 4.4.1: Presents modeled source water values and temperature for the first 50 years of our record using Eq 3.2 ($\delta^{18}O_{xw}$ (Roden)), Eq 3.3 (δD_{xw} (Roden)), and Eq 3.4 ($\delta^{18}O_{sw}$ (Anderson); Temp. (Anderson); Temp. (Roden)). Note the unrealistic values calculated for annual temperature Temp. (Anderson). Averages for the entire 203 year record are presented at the bottom.

Temperatures calculated using annual source water values derived from the Roden et al. (2000) equation obtained a temperature estimate of 13.4° C much closer to the 14.4° C derived from the gastropod shells. Given the large number of inferred values and assumptions needed for these calculations these modeled values must be carefully interpreted in a palaeoclimatic context. Much work still needs to be done to establish a reliable palaeoclimatic model for tree-ring isotope values.

5. Discussion

5.1 Dendroclimatology

Narrow growth rings, and the short twisted growth patterns of the trunk indicate a tree-line type vegetation, providing evidence of a boreal setting close to the northern tree-line. Changes in tree-ring width, in the Boreal Forest, has been assumed to be associated with changes in temperature, wider rings representing warm and narrow rings representing cold periods (Briffa, 2000). Warm and cold periods inferred from the tree-ring characteristics are shown in figure 4.2.1. Because the reduction in ring width at year 80 is most likely not an indication of temperature change significant peaks and troughs, differing from the average ring width after year 80, were used. However, uncertainty still exists as to how much of this signal is temperature-related and how much is atributable to water availability, light availability, nutrient availability and other factors. Thus, we have analyzed stable isotopes from the tree-rings to provide further data for interpretation.

5.2 Palaeoenvironmental signals

5.2.1 Carbon isotopes

Much research has compared tree-ring isotope values with climate data in an effort to ascertain which climate signals provide the dominant influence on the various isotope ratios (Leavitt and Long, 1991; Saurer *et al*., 1995; Anderson *et al*., 1998; Bowling *et al*., 2002; Liu *et al.*, 2004). In addition to climatic factors, many physiological factors also influence tree ring isotope values. Originally $\delta^{13}C$ values were thought to correspond to temperature, and indeed many authors have noted correlations between $\delta^{13}C$ values and summer temperature, even interpreting $\delta^{13}C$ values as changing by a

certain amount per degree Celsius (e.g. Leavitt and Long, 1991; Lipp *et al.*, 1991; Anderson *et al.*, 1998). Recent studies refute $\delta^{13}C$ as a palaeothermometer (Stewart, *et al.,* 1995; Warren *et al.,* 2001; Gagen *et al.,* 2004; Anderson *et al*., 2005). The apparent temperature signal is likely indirect, resulting from the influence of factors other than temperature on $\delta^{13}C$. Hot summers have a tendency to be dry, resulting in a correlation between temperature, RH (relative humidity) and soil water. Both RH and soil water directly influence stomatal conductance and therefore also control $\delta^{13}C$ values. Additionally, light intensity and summer temperature are also correlated, and irradiance influences photosynthetic rate that in turn affects $\delta^{13}C$ values. McCarroll and Pawellek (2001) found that $\delta^{13}C$ values of *Pinus* from moist sites in Finland were correlated with average hours of summer sunlight.

Edwards *et al*. (2000) attempted to resolve some of these difficulties by using a bi-variate approach, plotting isotope ratios in 'RH – T space'. McCarroll and Loader (2004) and Anderson *et al*. (2005) have argued that Edwards *et al.* (2000) bi-variate approach is not much of an improvement on the classical correlative approach to interpretation of isotope values because it only considers two of the primary environmental factors influencing $\delta^{13}C$ ratios.

Because $\delta^{13}C$ values in wood cellulose are strongly mediated by stomatal conductance, researchers have recently turned to $\delta^{13}C$ values as a proxy for soil water, relative humidity and photosynthetic rate (Leavitt, 2002; McCarroll and Loader, 2004). Higher $\delta^{13}C$ values imply drier conditions, and/or a higher photosynthetic rate, while lower $\delta^{13}C$ values suggest wet conditions, and/or a lower photosynthetic rate.

Fluctuations in warm/wet, warm/dry, cold/wet and cold/dry conditions could

reflect different phases associated with climate cycles and are shown in figure 5.2.1. Because $\delta^{18}O_{cellulose}$ values in reflect precipitation and evaporation, isotope values can be used to infer temperature and precipitation, while δD_{CN} has been used primarily as a proxy for temperature (Feng and Epstein, 1994). $\delta^{13}C_{cellulose}$ values serve as a proxy for wet and dry conditions (Leavitt and Long, 1991; Warren *et al*., 2001; Gagen *et al.,* 2004). Lastly, tree-ring widths provide an additional temperature proxy, although precipitation may also influence the widths of the rings. The record shows a prolonged wet period from year 98 to 137. This likely reflects a period of stable climate where perhaps the decadal scales cycles similar to the Arctic Oscillation (AO)/North Atlantic Oscillation (NAO) existed in a positive phase resulting in a warmer and wetter Arctic environment. Two dry periods near the end of the record (138-160; 174-196) separated by a wet period (161-173). These dry periods may represent a phase shift in the NAO-like cycle to a negative phase, because Arctic climate tends to be cool and dry when the AO/NAO is in a negative phase.

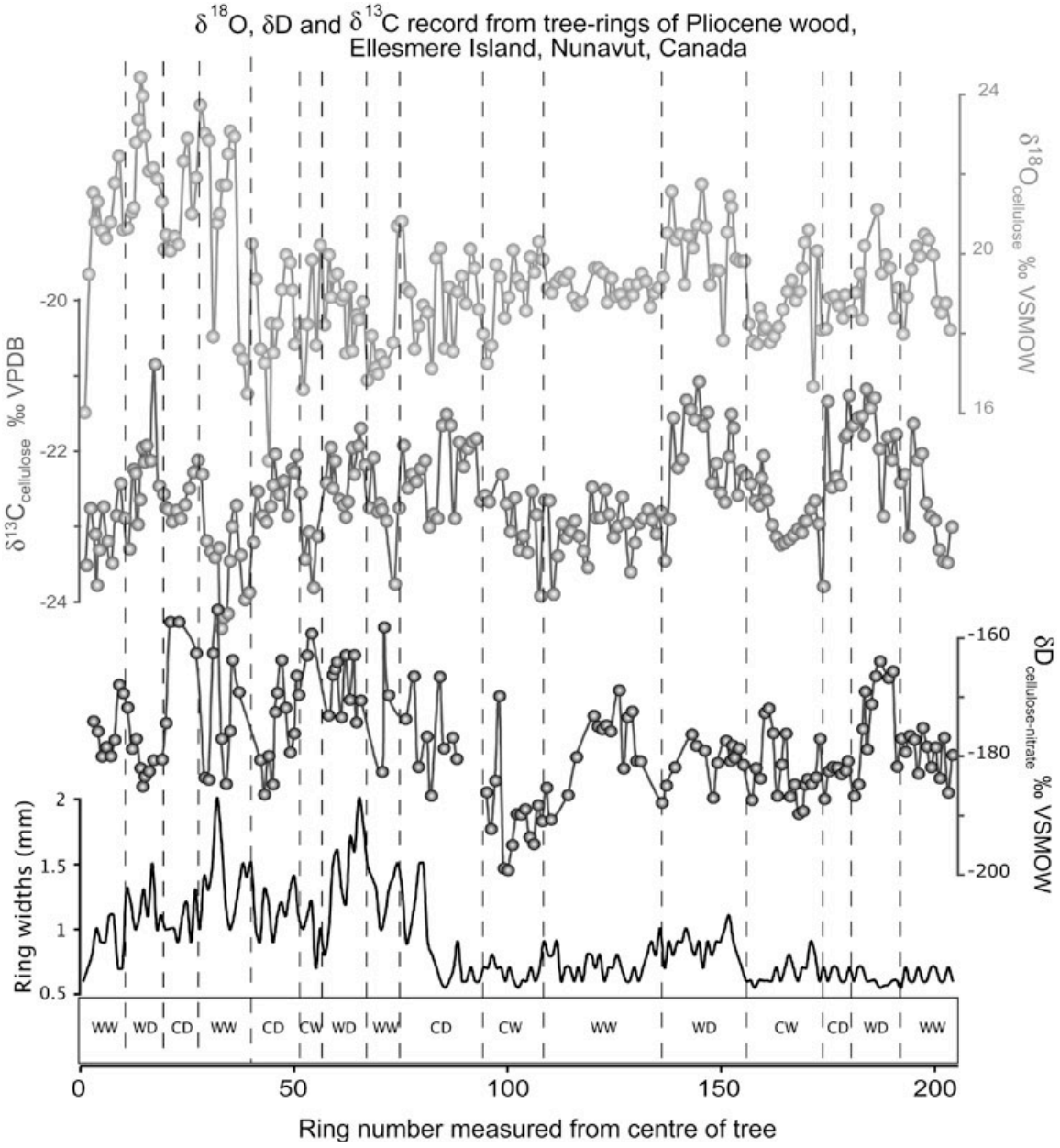

Figure 5.2.1: $\delta^{13}C$, $\delta^{18}O$, δD and ring width records from Pliocene log ELP-001. Climatic inferences are indicated along the bottom with WW= Warm/Wet, WD= Warm/Dry, CD= Cool/Dry, CW= Cool/Wet periods.

5.2.2 Water isotopes: Oxygen and Hydrogen

Feng and Epstein (1995) examined δD values of seven trees from six different locations in North America. Upon comparing δD values with instrumental records they noted a strong ($R^2 = 0.62$) correlation between the 5-year mean temperature and δD values. Tang *et al*. (2000) in a similar study from the Olympic Peninsula of Washington, noted a similar but weaker ($R^2 = 0.26$) correlation with temperature. They argued that the relationship between RH and temperature was the cause of this poor correlation. Roden *et al.* (2000) in a study conducted to find a non-correlative, model-based approach to interpretation of tree-ring $\delta^{18}O$ and $\delta^{13}C$ values, noted the importance of RH in the analysis of both isotopes and so incorporated it as a dominant factor in their modeling equation. Anderson *et al.* (2002) also incorporated RH into their model. Other studies argued that δD and $\delta^{18}O$ values reflect isotope values of precipitation and/or ground water (McCarroll and Loader, 2004). Several studies have found a strong correlation between precipitation and $\delta^{18}O_{cellulose}$ (Saurer *et al*., 1997; Robertson *et al*., 2001; Evans and Schrag, 2004), and δD values (Aucour *et al*., 2002; McCarroll and Loader, 2004). Despite promising results these correlations they are not useful in a palaeoclimatic context, because the degree of correlation varies greatly with location and depend on prior knowledge of climatic conditions. Additionally temperature, precipitation and RH are correlated with each other to the same degree that they correlate with tree-ring isotopes (Anderson *et al*., 1998), suggesting that perhaps the relationship between these factors and the isotope values is indirect rather than direct as suggested by other researchers. Factors such as the rapid increase of pCO_2 and the well known Seuss effect, the lowering of $\delta^{13}C_{air}$ values of atmospheric CO_2 in response to the burning of fossil

fuels (February and Stock, 1999; Waterhouse *et al*., 2004; McCarroll and Loader, 2004), may have different influences on $\delta^{13}C_{cellulose}$ values than past conditions. It is therefore impossible to use correlation studies that are not only site-specific but time-specific to provide any climatic information.

Because this study used a multi-proxy isotope approach coupled with tree ring widths we could draw on the dominant environmental signals present in all three isotopes to make inferences about climate. The dominant climatic signal reflected in tree-rings from boreal sites is temperature. δD is also believed to reflect temperature thus we can further interpret warm and cold periods can be further interpreted by examining periods where δD and ring-widths correlate. On a year-to-year basis it does not seem that the two records correlate very well. However, the general trends of the two records (Fig. 5.2.1) indicate that the two records show the same general trends indicating that a long-term temperature signal was recorded.

$\delta^{18}O$ in cellulose reflects precipitation and evaporation, therefore, $\delta^{18}O$ can be used as a record for temperature and precipitation. If it is warm and dry $\delta^{18}O$ values will be higher due to increased evaporation. If it is warm and wet there will likely be an increase but it will be much less. Cold and dry conditions likely will also result in a slight increase in $\delta^{18}O$ values while cold and wet conditions will reduce $\delta^{18}O$ values. $\delta^{13}C$ in cellulose reflects moisture stress and photosynthetic rate. Dry conditions will cause trees to close their stomates and thus $\delta^{13}C$ values will be higher. If conditions are wet trees will not close their stomates and consequently $\delta^{13}C$ values will be lower. Photosynthetic rate will likely not have a large effect on an annually resolved sample. δD has been used most frequently to infer temperature, thus we have used δD here as an additional check on our

temperature inferences. Figure 5.2.1 presents this multi-proxy reconstruction of warm/wet, cool/wet, warm/dry, cool/dry and moderate periods. This is an improvement on a single isotope approach since a multi-isotope approach allows the recognition of the differing environmental signals present in each isotope system as well as the different ways in which these environmental factors will influence each proxy.

5.2.3 Palaeoenvironmental modeling

Annual source water values calculated from $\delta^{18}O_{cellulose}$ if compared to modern Canadian precipitation isotope values are significantly higher than modern Ellesmere Island precipitation (average $\delta^{18}O_{precipitation}$ values of ~ –28 ‰). The $\delta^{18}O$ values cited here are closer to those recorded at the present tree-line (-16 to -22 ‰) in areas such as Whitehorse, YT or Yellowknife, NWT (CNIP, 2004).

Although the individual annual values calculated using the Anderson *et al*., (2002) equation, do not appear real (values range from –106 to 284° C), the average temperature works out to 11° C which is similar to the average growing season temperature of Whitehorse, YT (10.9° C) and Yellowknife, NWT (11.2° C).

Additionally if the $\delta^{18}O_{sw}$ value of –21.2 ‰ VSMOW calculated from the peat is plotted with the δD value calculated using the equation of Roden *et al*. (2000) the resulting point falls on the average polar meteoric water line, providing further evidence that these numbers may infact be a true reflection of Pliocene meteoric water isotope values.

5.3 Climate cycles

Time series wavelet analysis of isotope data and tree-ring widths reveals several cycles described below in terms of long-term (~25-50 year), intermediate (~10-16 year) and short-term (~5-8 year) periodicities and presented in (Figure 4.3.2). Long-term periodicities are some of the strongest periods present in the record and are recognized in all three isotope records, and appear as two dominant cycles. The strongest power in the wavelet spectrum occurs in the 25-50 year time band. The longest period cycle occurs at ~40 ($\delta^{13}C$), ~45 (δD) to ~50 ($\delta^{18}O$) years, and is a high power signal throughout the record in δD and $\delta^{18}O$ power spectra, while in the $\delta^{13}C$ the long-term periodicity is highest in power towards the end of the record, albeit extending beyond the cone of influence of the spectrum. A very distinct periodicity of ~30-35 years is recognized in all three isotope records, and is also a prominent feature of the ring-width record. Ring-width data record short (<10 yr), intermediate (~10-20 yr) and long (25-50 yr) periodicity.

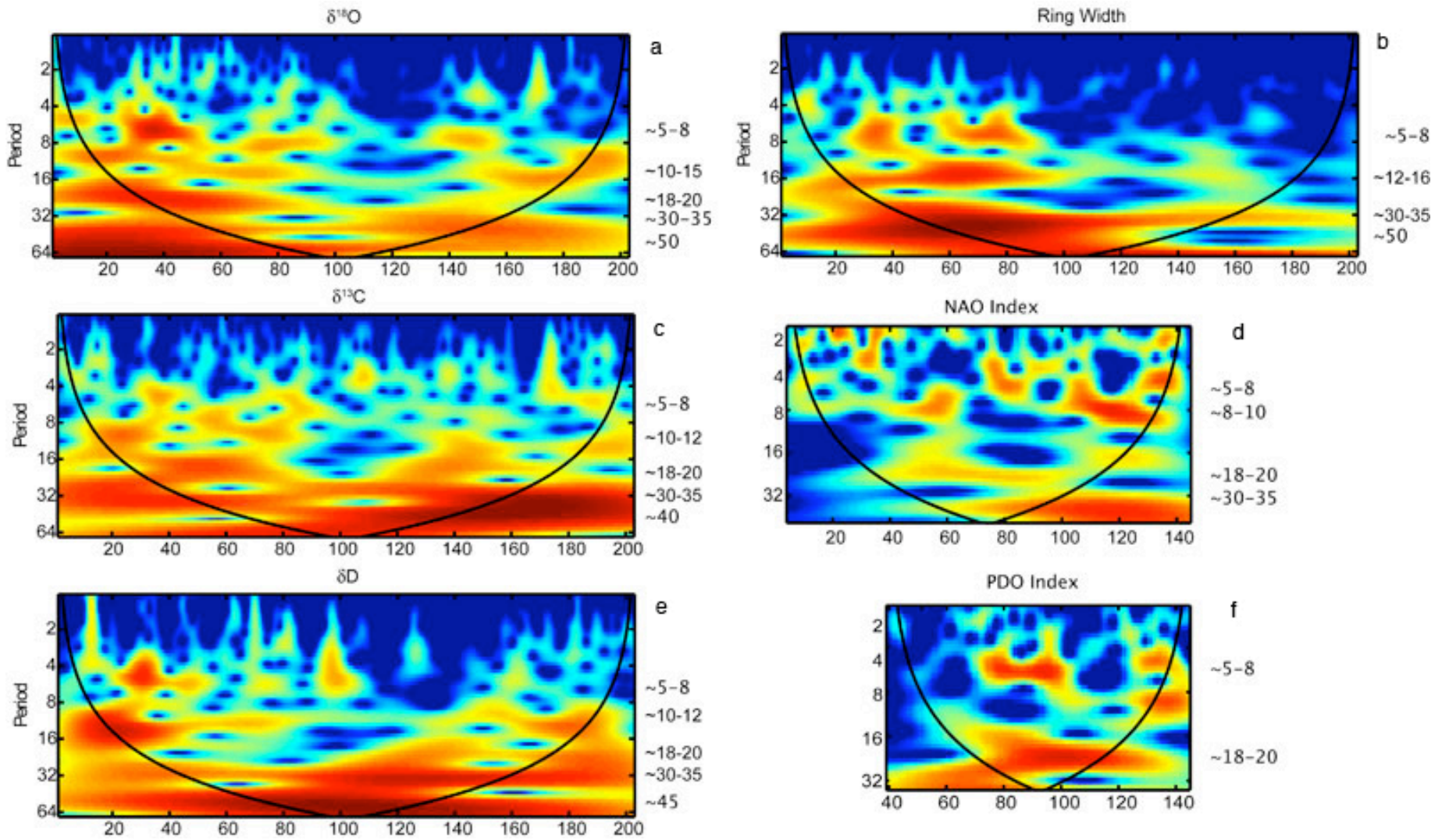
δ18O
a
Period
2
4
8
16
32
64
20 40 60 80 100 120 140 160 180 200
~5-8
~10-15
~18-20
~30-35
~50
Ring Width
b
Period
2
4
8
16
32
64
20 40 60 80 100 120 140 160 180 200
~5-8
~12-16
~30-35
~50
δ13C
c
Period
2
4
8
16
32
64
20 40 60 80 100 120 140 160 180 200
~5-8
~10-12
~18-20
~30-35
~40
NAO Index
d
2
4
8
16
32
20 40 60 80 100 120 140
~5-8
~8-10
~18-20
~30-35
δD
e
Period
2
4
8
16
32
64
20 40 60 80 100 120 140 160 180 200
~5-8
~10-12
~18-20
~30-35
~45
PDO Index
f
2
4
8
16
32
40 60 80 100 120 140
~5-8
~18-20

Figure 5.3.2: Wavelet analysis of Pliocene tree ring widths, isotope data and the NAO and PDO indices. All spectra have been adjusted to the same x and y scales to facilitate comparison. Prominent periodicity bands are indicated to the right of each spectrum. High power in the wavelet spectrum is indicated by red colours and low power by blues. NAO Index Data provided by the Climate Analysis Section, NCAR, Boulder, USA (Hurrell, 1995) PDO index data provided by the Joint Institute for the Study of the Atmosphere and Ocean at the University of Washington (Mantua and Hare, 2000).

Intermediate periodicity is intense in the first 90 years and again after 140 years in the $\delta^{13}C$ power spectrum as a period of ~10-12 years, $\delta^{18}O$ spectrum (~10-15 yr) and the early (0-90 year) part of the ring-with record (~12-16 yr). Although the signal is weak only in the δD spectrum is intermediate periodicity in the ~10-12 year band present during the quiet interval between year 90 and 140, although the signal is weak. A second intermediate cycle of 18-20 years is evident in the $\delta^{13}C$ and $\delta^{18}O$ spectra as well as the later part of the δD power spectrum.

Short periodicities are prominent features of all isotope power spectra but appear to be ephemeral. Greatest intensity appears sporadically at ~5-8 year periodicity, with decreased power in the 100-150 year interval. Short periodicity is also prominent in the ring-width power spectrum, but essentially disappears in the last half of the record.

The various data sets exhibit common power at several periods, as indicated by cross wavelet analysis (Fig. 5.3.3). Cross wavelet plots are derived by combining the signals present in two data sets to illustrate cycles common to both data sets. Figure 5.3.3 shows cross wavelet plots for Ring-width combined with each of the three isotope data sets (Fig 5.3.3 A-C), and each of the three isotope data sets compared with each other. The most prominent common power occurs within the 25-50 year band. There is a near constant ~35 year cycle in the ring width–$\delta^{13}C$ data. Periodicity decreases from ~48 years to ~35 years in the ring width–$\delta^{18}O$ data. The ~32 year periodicity is evident in the ring width–δD comparisons and in the $\delta^{13}C$–δD data; and a ~35 year cycle is evident in the $\delta^{18}O$–$\delta^{13}C$ data. Weak common power occurs in the $\delta^{18}O$–δD data sets at a ~32 year period, becoming stronger after 110 years. Intermittent intervals of common power at 3-

7 and ~16 year periodicity are also evident in all the data sets. This indicates that the strongest periodicities present in the record are in the 32-35 year and 16 year periods.

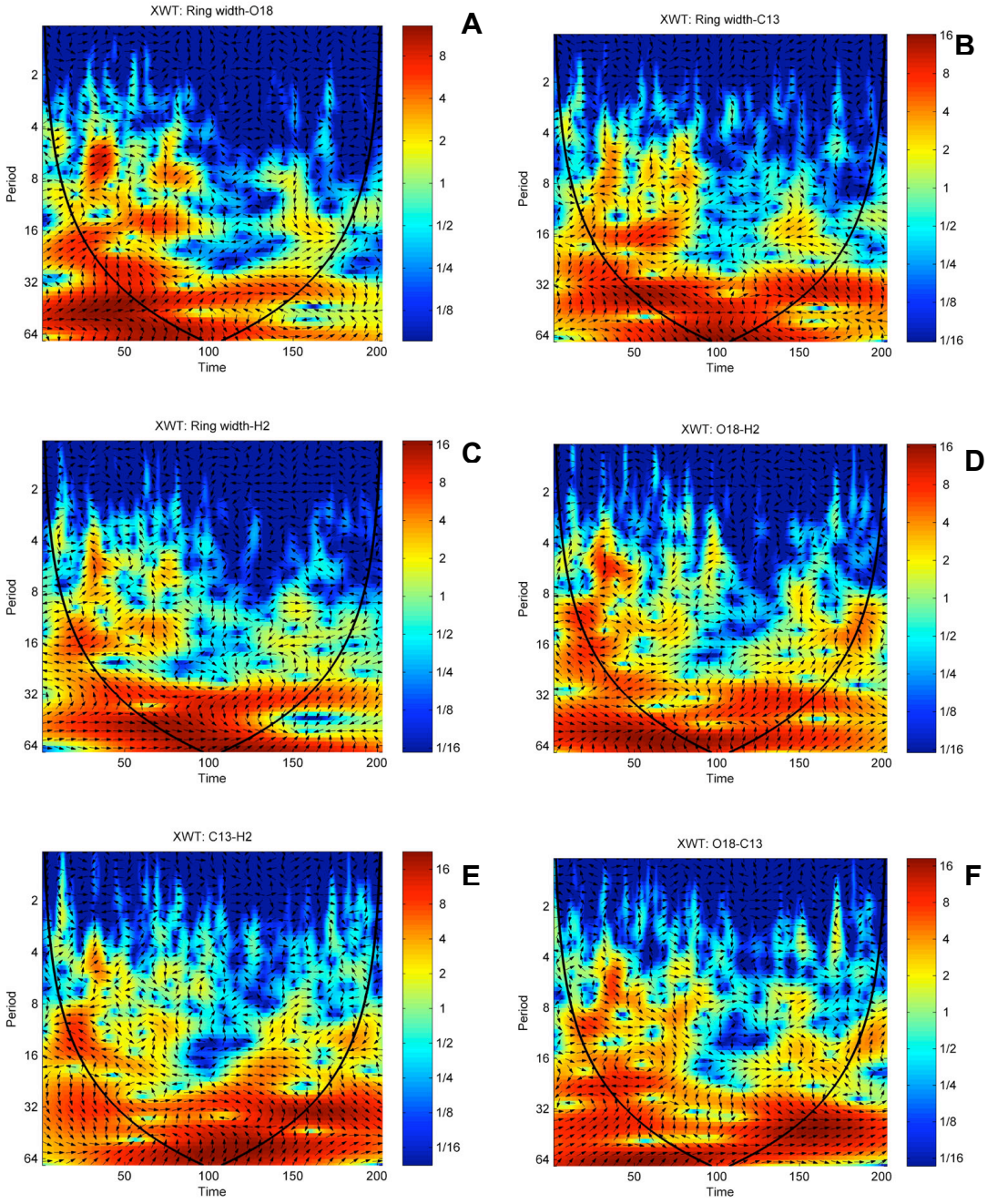

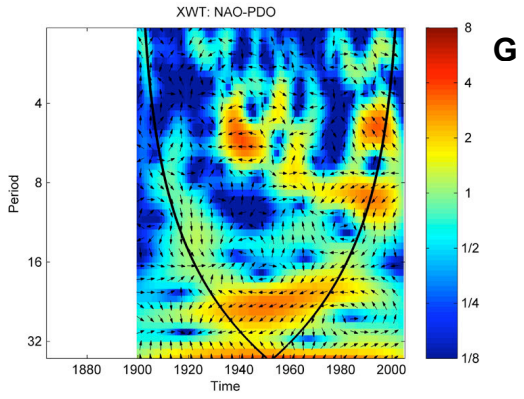

Figure 5.3.3: Presents cross wavelet analysis of all time series. Cross wavelet analysis combines the individual wavelet analyses of two data sets into one time-series in order to elucidate cycles that are present in both records. A-C consists of isotope records combined with the ring-width record, D-F are comparisons of the isotope data and G is a cross wavelet analysis of the NAO and PDO data. High power is illustrated in reds while blues indicate low power spectra.

This isotope record is the first such high-resolution Pliocene record that displays cycles similar to several modern cycles. In the modern climate system, several climate cycles have been described from the instrumental record developed over the past 100 years. These include Solar cycles, ENSO, the Pacific Decadal Oscillation, the North Atlantic Oscillation/Arctic Oscillation (Hurrell, 1995; Briffa, 2000; Cook *et al*., 2002; Mantua and Hare, 2002; Briffa and Osborn, 2002; Esper *et al.*, 2002). Several of the aforementioned cycles appear to be present in the Early Pliocene record.

The Pacific Decadal Oscillation (PDO) operates with periodicities of 15-25 years and 50-70 years (Mantua and Hare, 2002) with warm and cold phases. During the warm phase sea surface temperatures in the Central Pacific are anomalously high resulting in stronger counterclockwise winds and drought in the Pacific Northwest, with drier than

normal conditions in Alaska and the high Arctic, during a cold phase PDO conditions are reversed (Mantua and Hare, 2002). PDO variability has been noted in tree-ring records (Gedlof and Smith, 2001; D'Arrigo *et al*., 2005), as well as salmon migration records and sea surface temperature records from the Northwest Pacific.

El Niño/Southern Oscillation (ENSO) well documented in modern instrumental records, operates on a 4-8 year cycle. In normal conditions, the trade winds blow towards the west across the tropical Pacific and sea-surface temperatures are about 8 °C higher in the west with cooler temperatures of the coast of South America, due to upwelling cold water. El Niño is the phase of the Southern Oscillation where the trade winds relax in the central and western Pacific reducing the degree of upwelling cutting off the nutrient supply and warming sea surface temperatures off the coast of Peru. The warmer sea surface temperatures result in increased rainfall on the west coast of North and South America. Conversely, La Nina occurs when trade winds increase resulting in increased upwelling and dryer conditions in the eastern Pacific. La Nina usually occurs in the year immediately following El Niño. There exists some evidence that El Niño may have been in operation during the Pliocene (Ravelo *et al*., 2006) therefore it is not surprising that other climate cycles known from modern records may have been present.

Evidence based on molluscan and algal distribution during the early Pliocene suggests that water moved into the Arctic Ocean from the Atlantic and then southward to the Pacific through the Bering Strait, opposite of the conditions today (Marincovitch, 2000; Lindstrom, 2001). This implies that the Atlantic would have been the dominant influence on Arctic Ocean conditions at the time that our tree was growing suggesting that we should instead examine cycles present in the Atlantic Ocean.

The North Atlantic Oscillation (NAO) is a dominant climate mode of the Northern Hemisphere, transitioning with periodicities similar to those observed in the early Pliocene tree-ring isotope records. The NAO refers to a redistribution of atmospheric mass between the Arctic (centered on Iceland), and the subtropical Atlantic (centered on the Azores). The NAO swings from one phase to another producing large changes in mean wind speed and direction over the Atlantic, affecting heat and moisture transport between the ocean and the neighboring continents, as well as producing changes in the numbers and paths of storms (Hurrell *et al.*, 2003). When the NAO is positive, stronger northerly winds over Greenland and northeastern Canada carry cold air southward, thereby decreasing temperatures in the northwest Atlantic, opposite of a negative NAO (Hurrell *et al.*, 2003). It is particularly important to note such variations in climate as current research points to an increase in seasonality as one of the primary factors involved in late Pliocene glaciation of the Northern Hemisphere (Ravelo *et al.*, 2004; Haug *et al.*, 2005).

Subjecting the PDO and the NAO to wavelet analysis a 15-27 year and a faint 32-34 year cycle are revealed in the PDO index; however, the instrumental record of the PDO is to short to clearly demonstrate this longer period cycle, the NAO index shows a 14-20 year cycle as well as a 35-40 year cycle (Fig. 5.3.2).

The most prominent cycles in our record also appear to be present in the NAO and PDO records, suggesting that perhaps one or both of these cycles were operating as long ago as 4 to 5 million years ago. Recent tree-ring and other multi-proxy studies of climate on scales as long as 600 years have also begun to reveal that the NAO may have been present for at least as long as we have proxies at a high enough resolution to detect

it (Cook *et al.*, 2002). Past studies of climate have also revealed several other records of climate cyclicity with a period of ~30 years. In 1890 Brückner was the first to recognize a 30-35 year cycle in the climatic record (Brückner, 1890). Other records with ~30-year periodicity include the Fennoscandian tree-ring record (Briffa, 2000), the Galapagos coral oxygen isotope record (Dunbar *et al*., 1994) and the Kaplan sea surface temperature (SST) anomalies (Kaplan *et al*., 1998), as well as being present in both the NAO and PDO indices.

6. Conclusions

Trunk morphology and palaeoecology of the site, located at Strathcona Fiord, Ellesmere Island, suggest that during the Pliocene this locality was a tree-line environment located at the northern edge of and ancient Boreal Forest.

Identification of the specimen collected at the site was conducted using anatomical features of the wood. These wood anatomical characteristics combined with abundant cones and leaves present at the site indicate that the specimen is a pinaceous conifer belonging to the genus *Larix*.

This study presents the first multi-isotope study (δD, $\delta^{18}O$ and $\delta^{13}C$) of Pliocene fossil wood providing a detailed sub-annual to annual record. The multi-proxy record illustrates fluctuations in climate during the lifetime of the fossil tree, indicating periods of warm/wet, cold/wet, cold/dry and warm/dry conditions. These fluctuations in climatic conditions may be related to phase changes in the decadal-scale climate cycles operating at the time.

This study has revealed several high-resolution climate cycles, the highest ever reported for the pre-Holocene. The presence of these climate cycles provides evidence for decadal scale cyclicity similar to the modern NAO or PDO operating during the Early Pliocene. This is the first time cycles of this sort have been identified during the Pliocene and provides valuable new insight into these climate cycles and their importance in past climate.

This study also illustrates the value of a multi-proxy approach of climate reconstruction from tree-rings, particularly in light of the fact that only two of the prominent cycles in our record are present in the tree-ring width record.

Future studies of this type should provide additional evidence that high-resolution climate cycles, such as the NAO, PDO and ENSO, have been operating for far longer than our records indicate and are not limited to the modern system.

7. References

Anderson, W.T., Bernasconi, S.M., McKenzie, J.A. and Saurer, M., 1998. Oxygen and carbon isotopic record of climatic variability in tree ring cellulose (*Picea abies*): an example from central Switserland (1913-1995). Journal of Geophysical Research, **103**, 31,625-31,636.

Anderson, W.T., Bernasconi, S.M., McKenzie, J.A., Saurer, M. and Schweingruber, F., 2002. Model evaluation for reconstructing the oxygen isotopic composition in precipitation from tree ring cellulose over the last century. Chemical Geology, **182**, 121-137.

Anderson, W.T., Sternberg, L.S.L., Pinzon, M.C., Gann-Troxler, T., Childers, D.L. and Duever, M., 2005. Carbon isotopic composition of cypress trees from South Florida and changing hydrologic conditions. Dendrochronologia, **23** (1), 1-10.

Aucour, A.-M., Tao, F.-X., Sheppard, S.M.F., Huang, N.-W. and Liu, C.Q., 2002. Climatic and monsoon isotopic signals (δD, $\delta^{13}C$) of northeastern China tree rings. Journal of Geophysical Research, **107**, 10.1029/2001JD000464.

Baillie, M.G., Pilcher, J.R., Pollard, A.M., and Ramesh, R., 2000. Climatic significance of D/H and $^{13}C/^{12}C$ ratios in Irish oak cellulose. Proceedings of the Indian Academy of Science, **109** (1), 117-127.

Barbour, M.M., Walcroft, A.S., and Farquhar, G.D., 2002. Seasonal variation in $\delta^{13}C$ and $\delta^{18}O$ of cellulose from growth rings of *Pinus radiata*. Plant, Cell and Environment, **25**, 1483-1499.

Beerling, D.J., 1998. The future as the key to the past for paleobotany?. Trends in Ecology and Evolution, **13** (8), 311-316.

Berggren, W.A., and Prothero, D.R., 1992. Eocene-Oligocene climatic and biotic evolution: an overview, *In*: Prothero, D.R., and Berggren, W.A., (Eds.), Eocene-Oligocene climatic and biotic evolution. Princeton University Press, Princeton, pp. 1-28.

Bennike, O., Abrahamsen, N., Bak, M., Israelson, C., Konradi, P., Matthiessen, J., and Witkowski, A., 2002. A multi-proxy study of Pliocene sediments from Île de France, North-East Greenland. Palaeogeography, Palaeoclimatology, Palaeoecology, **186**, 1-23.

Bowling, D.R., McDowell, N.G., Bond, B.J., Law, B.E. and Ehleringer, J.R., 2002. ^{13}C content of ecosystem respiration is linked to precipitation and vapor pressure deficit. Oecologia, **131**, 113-124.

Brendel, O., Iannetta, P.P.M., and Stewart, D., 2000. A rapid and simple method to isolate pure alpha-cellulose. Phytochemical Analysis, **11**, 7-10.

Briffa, K. R., 2000, Annual climate variability in the Holocene: interpreting the message of ancient trees. Quaternary Science Reviews, **19**, 87-105.

Briffa, K.R., and Osborn, T., 2002. Blowing hot and cold. Science, **295**, 2227-2228.

Brückner, E., 1890, Klimaschwankungen seit 1700 nebst Bemerkungen über die Klimaschwankungen der Diluvialzeit: Geographische Abhandlungen herausgegeben 325 pp.

CNIP. (2004, October 29th). *Canadian Network for Isotopes in Precipitation*. [wwwdocument] URL: http://www.science.uwaterloo.ca/~twdedwar/cnip/cniphome.html

Cook, E.R., Buckley, B.M., D'Arrigo, R.D. and Peterson, M.J., 2000. Warm-season temperatures since 1600 B.C. reconstructed from Tasmanian tree rings and their relationship to large-scale sea surface temperature anomalies. Climate Dynamics, **16** (2/3), 79-91.

Cook, E.R., D'Arrigo, R.D. and Mann, M.E., 2002. A well-verified, multiproxy reconstruction of the winter North Atlantic Oscillation index since A.D. 1400. Journal of Climate, **15**, 1754-1764.

Creber, G.T., 1977. Tree rings: a natural data-storage system. Biological Review, **52**, 349-383.

Creber, G.T. and Chaloner, W.G., 1985. Tree growth in the Mesozoic and Early Tertiary and the reconstruction of paleoclimates. Palaeogeography, Palaeoclimatology, Palaeoecology, **52**, 35-60.

Creber, G.T., and Francis, J.E., 1999. Fossil tree-ring analysis: palaeodendrology. *In* Jones, T.P. and Rowe, N.P [Eds.] Fossil plants and spores: modern techniques. Geological Society, London, pp. 245-250.

D'Arrigo, R., Mashig, E., Frank, D., Wilson, R. and Jacoby, G., 2005. Temperature variability over the past millennium infered from Northwestern Alaska tree rings. Climate Dynamics, **24**, 227-236.

Demske, D., Mohr, B., and Oberhänsli, H., 2002. Late Pliocene vegetation and climate of the Lake Baikal region, southern East Siberia, reconstructed from palynological data. Palaeogeography, Palaeoclimatology, Palaeoecology, **184**, 107-129.

Diester-Haass, L. and Zahn, R., 1996, The Eocene-Oligocene transition in the Southern Ocean: history of water masses, circulation, and biological productivity inferred

from high resolution records of stable isotopes and benthic foraminiferal abundances (ODP Site 689). Geology, **24**, 16-20.

Dowsett, H.J., Barron, J., and Poore, R.Z., 1996. Middle Pliocene sea surface temperatures. A global reconstruction. Marine Micropaleontology, **27,** 13-25.

Dunbar, R. B., Wellington, G. M., Colgan, M. W., and Glynn, P. W., 1994. Eastern Pacific sea surface temperature since 1600 A. D.: the $\delta^{18}O$ record of climate variability in Galapagos corals. Paleoceanography, **9**, 291-315.

Edwards, L.E., Mudie, P.J., and de Vernal, A., 1991. Pliocene paleoclimatic reconstructions using dinoflagellate cysts: comparison of methods. Quaternary Science Reviews, **10**, 259-274.

Edwards, T.W.D., Graf, W., Trimborn, P., Stichler, W., Lipp, J. and Payer, H.D., 2000. $\delta^{13}C$ response surface resolves humidity and temperature signals in trees. Geochimica et Cosmochimica Acta, **64**, 161-167.

Ekart, D.D., Cerling, T.E., Montañez, I.P. and Tabor, N.J., 1999. A 400 million year carbon isotope record of pedogenic carbonate: implications for paleoatmospheric carbon dioxide. American Journal of Science, **299**, 805-827.

Esper, J., Cook, E.R., and Schweingruber, F.H., 2002. Low-Frequency signals in long tree-ring chronologies for reconstructing past temperature variability. Science, **295**, 2250-2253.

Evans, M.N. and Schrag, D.P., 2004. A stable isotope-based approach to tropical dendroclimatology. Geochimica et Cosmochimica Acta, **68**, 3295-3305.

February, E.C. and Stock, W. D., 1999. Declining trend in the $^{13}C/^{12}C$ ratio of atmospheric carbon dioxide from tree rings of South African *Widdringtonia cedarbergensis*. Quaternary Research, **52**, 229-236.

Feng, X. and Epstein, S., 1995. Climatic temperature records in δD data from tree rings. Geochimica et Cosmochimica Acta, **59** (14), 3029-3037.

Flesche Kleiven, H., Jansen, E., Fronval, T., and Smith, T.M., 2002. Intensification of Northern Hemisphere glaciations in the circum Atlantic region (3.5-2.4 Ma) – ice-rafted detritus evidence. Palaeogeography, Palaeoclimatology, Palaeoecology, **184**, 213-223.

Francis, J.E. and Hill, R.S., 1996. Fossil plants from the Pliocene Sirius Group, Transantarctic Mountains: evidence for climate from growth rings and fossil leaves. Palaios, **11**, 389-396.

Funder, S., Bennike, O., Böcher, J., Israelson, C., Petersen, K.S., and Símonarson, L.A., 2001. Late Pliocene Greenland – the Kap København formation in North Greenland. Bulletin of the Geological Society of Denmark, **48**, 117-134.

Fyles, J.G., McNeil, D.H., Matthews Jr., J.V., Barendregt, R.W., Marincovich Jr., L., Brouwers, Bednarski, J., Brigham-Grette, J., Ovenden, L.E., Miller, K.G., Baker, and J., Irving, E., 1998. Geology of Hvitland Beds (late Pliocene), White Point Lowland, Ellesmere Island, Northwest Territories. Geological Survey of Canada Bulletin, **512**, pp. 14-23.

Fyles, J.G., Marincovich Jr., L., Matthews Jr., J.V., and Barendregt, R., 1991. Unique mollusc find in the Beaufort Formation (Pliocene) on Meighen Island, Arctic Canada; *In* Current Research, Part B, Geological Survey of Canada, **91-1B**, 105-112.

Fyles, J.G., 1990. Beaufort Formation (late Tertiary) as seen from Prince Patrick Island, Arctic Canada. Arctic, **43** (4), 393-403

Fyles, J.G., 1989. High terrace sediments, probably of Neogene age, west-central Ellesmere Island, Northwest Territories. *In* Current Research, Part D, Geological Survey of Canada, **89-1D**, 101-104.

Gagen, M., McCarroll, D. and Edouard, J.L., 2004. Latewood width, maximum density and stable carbon isotope ratios of pine as climate indicators in a dry subalpine environment. Arctic, Antarctic and Alpine Research, **36** (2), 166-171.

Gedalof, Z. and Smith, D.J. 2001. Interdecadal climate variability and regime-scale shifts in Pacific North America. Geophysical Research Letters, **28**, 1515-1518.

Glerum, C. and Farrar, J.L., 1966. Frost ring formation in the stems of some coniferous species. Canadian Journal of Botany, **44**, 879-886.

Grindted, A., Moore, C.H. and Jevrejeva, S., 2004. Application of the cross wavelet transform and wavelet coherence to geophysical time series. Nonlinear Processes in Geophysics, **11**, 561-566.

Hare, F.K., and Ritchie, J.C. 1972. The boreal bioclimates. Geogr. Rev. 62: 333-365.

Haug, G.H., Ganopolski, A., Sigman, D.M., Rosell-Mele, A., Swann, G.E.A., Tiedemann, R., Jaccard, S.L., Bollmann, J., Maslin, M.A., Leng, M.J. and Eglinton, G., 2005. North Pacific seasonality and the glaciation of North America 2.7 million years ago. Nature, **433**, 821-825.

Haywood, A.M., and Valdes, P.J., 2004. Modelling Pliocene warmth: contribution of atmosphere, oceans and cryosphere. Earth and Planetary Science Letters, **218**, 363-377.

Haywood, A.M., Valdes, P.J., and Sellwood, B.W., 2002. Magnitude of climate variability during middle Pliocene warmth: a palaeoclimate modelling study. Palaeogeography, Palaeoclimatology, Palaeoecology, **188**, 1-24.

Haywood, A.M., Valdes, P.J., and Sellwood, B.W., 2000. Global scale palaeoclimate reconstruction of the middle Pliocene climate using the UKMO GCM: initial results. Global Planetary Change, **25**, 239-256.

Hill, R.S., Harwood, D.M., and Webb, P.N., 1996. Nothofagus beardmorensis (Nothofagaceae), a new species based on leaves from the Pliocene Sirius Group, Transantarctic Mountains, Antarctica. Review of Palaeobotany and Palynology, **94**, 11-24.

Houghton, J.T., Meira-Filho, L.G., Callander, B.A., Harris, N., Kattenberg, A., and Maskell, K., 1996. Climate change 1995 – the science of climate change: the second assessment report of the Intergovernmental Panel on Climate Change. Cambridge University Press.

Hulbert Jr., R.C., and Harington, C.R., 1999. An early Pliocene hipparionine horse from the Canadian Arctic. Palaeontology, **42**, 1017-1025.

Hurrell, J. W., 1995, Comparison of NCAR Community Climate Model (CCM) climates. Climate Dynamics, **11**, 25-50.

Hurrell, J. W., Kushnir, Y., Ottersen, G. and Visbeck, M., 2003, The North Atlantic Oscillation: Climatic Significance and Environmental Impact. Geophysical Monographs 134, Washington, D.C., American Geophysical Union, pp. 1-35.

Ivany, L.C., Nesbitt, E.A., and Prothero, D.R., 2003. The marine Eocene-Oligocene transition: a synthesis. *In*: Prothero, D.R., Ivany, L.C., Nesbitt, E.A. (Eds.) From greenhouse to icehouse the marine Eocene-Oligocene transition. Columbia University Press, New York, pp. 522-534.

Ivany, L.C., Patterson, W.P., and Lohmann, K.C., 2000. Cooler winters as a possible cause of mass extinctions at the Eocene/Oligocene boundary. Nature, **407**, 887-890.

Jahren, A.H., and Sternberg, L.S.L., 2003. Humidity estimate for the middle Eocene Arctic rain forest. Geology, **31**, 463-466.

Jane, F.W., 1970. The Structure of wood. Adam & Charles Black, London.

Kaplan, A., Cane, M., Kushnir, Y., Clement, A., Blumenthal, M., and Rajagopalan, 1998. Analyses of global sea surface temperature 1856-1991. Journal of Geophysical Research, **103**, 18,567-18,589.

Kurschner, W.M., vanderBurgh, J., Visscher, H., and Dilcher, D.L., 1996. Oak leaves as biosensors of late Neogene and early Pleistocene paleoatmospheric CO2 concentrations. Marine Micropaleontology, **27** (1-4), 299-312.

Leavitt, S.W., 2002. Seasonal response of $\delta^{13}C$ in *Pinus resinosa* Ait. seedling growth rings to changing environment in controlled growth experiments. Dendrochronologia, **19** (1), 9-22.

Leavitt, S.W. and Long, A., 1991. Seasonal stable-carbon isotope variability in tree-rings: possible paleoenvironmental signals. Chemical Geology (Isotope Geoscience Section), **87**, 59-70.

Lindstrom, S.C., 2001. The Bering Strait connection: dispersal and speciation in boreal macroalgae. Journal of Biogeography, **28**, 243-251.

Lipp, J., Trimborn, P., Fritz, P., Moser, H., Becker, B. and Frenzel, B., 1991. Stable isotopes in tree-ring cellulose and climatic change. Tellus, **43B**, 322-330.

Liu, Y., Ma, L., Leavitt, S.W., Cai, Q. and Liu, W., 2004. Seasonal precipitation reconstruction from tree-ring stable carbon isotopes at Mt. Helan, China, since AD 1804. Global and Planetary Change, **41**, 229-239.

Loader, N.J., Robertson, I., Barker, A.C., Switsur, V.R., and Waterhouse, J.S., 1997. A modified method for the batch processing of small whole wood samples to α-cellulose. Chemical Geology, **136**, 313-317.

Manjoube, M., 1971. Fractionnement en oxygène 18 et en deuterium entre l'eau et sa vapeur. Journal Chimie Physique, **68**, 1423-1436.

Mantua, N. J. and Hare, S. R., 2002. The Pacific decadal oscillation. Journal of Oceanography, **58**, 35-44.

Marincovich, L. (Jr.), 2000. Central American paleogeography controlled Pliocene Arctic Ocean molluscan migrations. Geology, **38**, 151-154.

Maslin, M.A., Haug, G.H., Sarnthein, M., and Tiedemann, R., 1996. The progressive intensification of Northern Hemisphere glaciation as seen from the North Pacific. Geologisch Rundsch, **85**, 452-465.

Matthews Jr., J.V., and Ovenden, L.E., 1990. Late Tertiary plant macrofossils from localities in Arctic/Subarctic North America: a review of the data. Arctic, **43** (4), 364-392.

Matthews Jr., J.V., Ovenden, L.E., and Fyles, J.G., 1990. Plant and insect fossils from the late Tertiary Beaufort Formation on Prince Patrick Island, N.W.T. *In*: Harington,

C.R. (Ed.), Canada's missing dimension: science and history in the Canadian Arctic Islands. Canadian Museum of Nature, Ottawa, pp. 105-139.

Meylan, B.A., 1972, Thre-dimensional structure of wood: a scanning electron microscope study. Chapman and Hall, London.

Miall, A.D., 1986. The Eureka Sound Group (Upper-Cretaceous-Oligocene), Canadian Arctic Islands. Bulletin of Canadian Petroleum Geology, **34**, 240-270.

McCarroll, D., and Loader, N.J., 2004. Stable isotopes in tree rings. Quaternary Science Reviews, **23**, 771-801.

McIver, E.E., and Basinger, J.F., 1999. Early Tertiary floral evolution in the Canadian High Arctic. Annals of the Missouri Botanical Garden, **86**, 523-545.

Moritz, R.E., Bitz, C.M. and Steig, E.J., 2002. Dynamics of recent climate change in the Arctic. Science, **297**, 1497-1502.

Overpeck, J., Hughen, K., Hardy, D., Bradley, R., Case, R., Douglas, M., Finney, B., Gajewski, K., Jaboby, G., Jennings, A., Lamoureux, S., Lasca, A., MacDonald, G., Moore, J., Retelle, M., Smith, S., Wolfe, A., and Zielinski, G., 1997, Arctic Environmental Change for the Last Four Centuries. Science, **278**, 1251-1256.

Patterson, W.P., Smith, G.R. and Lohmann, K.C., 1993. Continental paleothermometry and seasonality using the isotopic composition of aragonitic otoliths of freshwater fishes, *in* Swart, P., Lohmann, K.C., McKenzie, J. and Savin, S. (eds.) American Geophysical Union Monograph Continental Climate Change from Isotopic Indicators, pp. 191-202.

Pagani, M., Zachos, J.C., Freeman, K.H., Tipple, B. and Bohaty, S., 2005. Marked decline in atmospheric carbon dioxide concentrations during the paleogene. Science, **309**, 600-603.

Pearson, P.N., and Palmer, 1999. Middle Eocene seawater pH and atmospheric carbon dioxide concentrations. Science, **284**, 1824-1826.

Pole, M., 2003. New Zealand climate in the Neogene and implications for global atmospheric circulation. Palaeogeography, Palaeoclimatology, Palaeoecology, **193**, 269-284.

Ravelo, A.C., Andreasen, D.H., Lyly, M., Lyle, A.O. and Wara, M.W., 2004. Regional climate shifts caused by gradual global cooling in the Pliocene epoch. Nature, **429**, 263-267.

Raymo, M.E., Grant, B., Horowitz, M. and Rau, G.H., 1996. Mid-Pliocene warmth: stronger greenhouse and stronger conveyor. Marine Micropaleontology, **27**, 313-326.

Ricketts, B.D. and Stephenson, R.A., 1994. The demise of the Sverdrup Basin: Late Cretaceous-Paleogene sequence stratigraphy and forward modeling. Journal of Sedimentary Research, **B64** (4), 516-530.

Robertson, I., Waterhouse, J.S., Barker, A.C., Carter, A.H.C. and Switsur, V.R., 2001. Oxygen isotope ratios of oak in east England: implications for reconstructing the isotopic composition of precipitation. Earth and Planetary Science Letters, **191**, 21-31.

Roden, J.S. and Ehleringer, J.R. 2000. Hydrogen and oxygen isotope ratios of tree ring cellulose for field-grown riparian trees. Oecologia, **123**, 481-189.

Roden, J.S., Lin, G., and Ehleringer, J.R., 2000. A mechanistic model for interpretation of hydrogen and oxygen isotope ratios in tree-ring cellulose. Geochimica et Cosmochimica Acta, **64**, 21-35.

Royer, D.L., Wing, S.L., Beerling, D.J., Jolley, D.W., Koch, P.L., Hickey, L.J., and Berner, R.A., 2001. Paleobotanical evidence for near present-day levels of atmospheric CO_2 during part of the Tertiary. Science, **292**, 2310–2313

Ruddiman, W.F., 2001. Earth's climate past and future. W.H. Freeman and company, pp. 414-418.

Saurer, M., Siegenthaler, U. and Schweingruber, F., 1995. The climate-carbon isotope relationship in tree rings and the significance of site conditions. Tellus, **47B**, 320-330.

Saurer, M., Borella, S. and Leuenberger, M., 1997. $\delta^{18}O$ of tree rings of beech (*Fagus silvatica*) as a record of $\delta^{18}O$ of the growing season precipitation. Tellus, **49B**, 80-92.

Saurer, M., Aellen, K., and Siegwolf, R., 1997. Correlating $\delta^{13}C$ and $\delta^{18}O$ in cellulose of trees. Plant Cell and Environment, **20**, 1543-1550.

Shackleton, N.J., Hall, M.A., and Pete, D., 1995. Pliocene stable isotope stratigraphy of site 846. *In*: Pisias, N.G., Mayer, L.A., Janecsek, T.R., Palmer-Julson, A., van Andel, T.H. (Eds.), Proc. ODP Sci. Results, **138,** pp. 223-237.

Shackleton, N.J., Backman, J., Zimmerman, H., Kent, D.V., Hall, M.A., Roberts, D.G., Schnitker, D., Baldauf, J.G., Desprairies, A., Homrighausen, R., Huddlestun, P., Keene, J.B., Kaltenback, A.J., Krumsiek, K.A.O., Morton, A.C., Murray, J.W., and Westberg-Smith, J., 1984. Oxygen isotope calibration of the onset of ice-

rafting and history of glaciation in the North Atlantic region. Nature, **307**, 620-623.

Sigman, D.M., Jaccard, S.L., and Haug, G.H., 2004. Polar ocean stratification in a cold climate. Nature, **428**, 59-63.

Sloan, L.C., Walker, J.C.G., Moore, T.C., Rea, D.K., and Zachos, J.C., 1992. Possible methane-induced polar warming in the early Eocene. Nature, **357**, 320–322.

Spicer, R.A., and Chapman, J.L., 1990. Climate change evolution of high-latitude terrestrial vegetation and floras. Trends in Ecology and Evolution, **5** (9), 279-284.

Stainforth, D.A., Aina, T., Christensen, C., Collins, M., Faull, N., Frame, D.J., Kettleborough, J.A., Knight, S., Martin, A., Murphy, J.M., Piani, C., Sexton, D., Smith, L.A., Spicer, R.A., Thorpe, A.J. and Allen, M.R., 2005, Uncertainty in predictions of climate response to rising levels of greenhouse gases. Nature, **433**, 403-406.

Sternberg, L.S.L., 1989. Oxygen and hydrogen isotope measurements in plant cellulose analysis. *In*: Linskens, H.F., Jackson, J.F. (Eds.), Modern methods of plant analysis, **10**, Springer-Verlag, Berlin, pp. 89-99.

Stewart, G.R., Turnbull, M.H., Shmidt, S. and Erskine, P.D., 1995. ^{13}C natural abundance in plant communities along a rainfall gradient: a biological integrator of water availability. Australian Journal of Plant Physiology, **22**, 51-55.

Tang, K., Feng, X. and Ettl, G.J., 2000. The variations in δD of tree rings and the implications for climatic reconstruction. Geochimica et Cosmochimica Acta, **64** (10), 1663-1673.

Tedford, R.H., and Harington, C.R., 2003. An Arctic mammal fauna from the early Pliocene of North America. Nature, **425**, 388-390.

Terwilliger, V.H., and DeNiro, M.J., 1995. Hydrogen isotope fractionation in wood-producing avocado seedlings: Biological constraints to paleoclimatic interpretations of δD values in tree ring cellulose nitrate. Geochimica et Cosmochimica Acta, **59**, 5199-5207.

Tiedemann, R., Sarnthein, M, and Shackleton, N.J., 1994. Astronomic timescale for the Pliocene Atlantic $\delta^{18}O$ and dust flux records of Ocean Drilling Program site 659. Paleoceanography, **9**(4), 619-638.

Torrence, C. and Compo, G.P., 1998. A practical guide to wavelet analysis. Bulletin of the American Meteorological Society, **79**, 61-78.

van Bergen, P.F., and Poole, I., 2002. Stable carbon isotopes of wood: a clue to palaeoclimate? Palaeogeography, Palaeoclimatology, Palaeoecology, **182**, 31-45.

Van Der Burgh, J., Visscher, H., Dilcher, D.L., and Kürschner, W.M., 1993. Paleoatmospheric signatures in Neogene fossil leaves. Science, **260**, 1788-1790.

Warren, C.R., McGrath, J.F. and Adams, M.A., 2001. Water availability and carbon isotope discrimination in conifers. Oecologia, **127**, 476-486.

Waterhouse, J.S., Switsur, V.R., Barker, A.C., Carter, A.H.C., Hemming, D.L., Loader, N.J. and Robertson, I., 2004. Northern European trees show a progressively diminishing response to increasing atmospheric carbon dioxide concentrations. Quaternary Science Reviews, **23**, 803-810.

Waterhouse, J.S., Switsur, V.R., Barker, A.C., Carter, A.H.C. and Robertson, I., 2002. Oxygen and hydrogen isotope ratios in tree rings: how well do models predict observed values? Earth and Planetary Science Letters, **201**, 421-430.

Williams, M., Haywood, A.M., Hillenbrand, C.D. and Wilkinson, I.P., 2005, Efficacy of $\delta^{18}O$ data from Pliocene planktonic foraminifer calcite for spatial sea surface temperature reconstruction: comparison with a fully coupled ocean-atmosphere GCM and fossil assemblage data for the mid Pliocene. Geological Magazine, **142**, 399-417.

Wilson, A.T., Grinsted, M.J., 1977. $^{12}C/^{13}C$ in cellulose and lignin as palaeothermometers. Nature, **265**, 133-135.

Zachos, J., Pagani, M., Sloan, L., Thomas, E., Billups, K., 2001. Trends, rhythms, and aberrations in global climate 65 Ma to present. Science, **292**, 686-690

Appendix A:

Raw isotope and tree-ring values

Ring ID	$\delta^{18}O$	Ring ID	$\delta^{13}C$	Ring ID	δD	Ring ID	Ring width (mm)
ELP-01A	15.9	ELP-01A	-23.1	ELP-02A	-177.2	ELP-01A	0.1
ELP-02A	19.4	ELP-02A	-22.3	ELP-03A	-179.1	ELP-02A	0.2
ELP-03A EW	22.1	ELP-03A EW	-22.7	ELP-04A	-183.7	ELP-03A	0.3
ELP-03A EW	21.0	ELP-03A LW	-23.4	ELP-05A	-182.0	ELP-04A	0.5
ELP-03A LW	20.8	ELP-04A	-22.9	ELP-06A	-183.6	ELP-05A	0.4
ELP-04A	21.4	ELP-05A	-22.3	ELP-06A	-179.4	ELP-06A	0.4
ELP-04A	21.2	ELP-06A	-22.8	ELP-07A	-181.5	ELP-07A	0.6
ELP-05A	20.7	ELP-07A	-23.1	ELP-07A	-179.8	ELP-08A	0.6
ELP-05A	20.4	ELP-08A	-22.4	ELP-08A	-170.5	ELP-09A	0.2
ELP-06A	20.7	ELP-09A	-22.0	ELP-09A	-172.3	ELP-10A	0.2
ELP-06A	20.0	ELP-10A	-22.4	ELP-09A	-171.9	ELP-11	0.8
ELP-07A	21.0	ELP-10A	-22.5	ELP-10A	-174.7	ELP-12	0.7
ELP-07A	20.5	ELP-01 EW	-22.9	ELP-11A	-181.5	ELP-13	0.5
ELP-08A	21.7	ELP-02 EW	-21.8	ELP-11A	-183.0	ELP-14	0.6
ELP-08A	21.9	ELP-02 LW	-21.9	ELP-12A	-180.3	ELP-15	0.8
ELP-09A	22.1	ELP-02 LW	-21.8	ELP-12A	-180.5	ELP-16	0.6
ELP-09A	22.8	ELP-03 EW	-22.5	ELP-02LW	-153.6	ELP-17	1
ELP-10A	20.4	ELP-03 LW	-22.2	ELP-13A	-185.8	ELP-18	0.5
ELP-10A	20.8	ELP-04 EW	-21.6	ELP-13A	-188.6	ELP-19	0.6
ELP-01	20.6	ELP-04 EW	-21.4	ELP-03EW	-165.1	ELP-20	0.5
ELP-02 EW	21.2	ELP-04 LW	-21.7	ELP-03LW	-189.2	ELP-21	0.5
ELP- 02 EW	20.8	ELP-05	-21.5	ELP-14A	-189.2	ELP-22	0.5
ELP-02 LW	20.6	ELP-06	-21.6	ELP-14A	-185.4	ELP-23	0.4
ELP-02 LW	21.7	ELP-06	-21.7	ELP-04EW	-161.3	ELP-24	0.6
ELP-03 EW	22.8	ELP-07	-20.3	ELP-04LW	-107.0	ELP-25	0.7
ELP-03 LW	23.4	ELP-07	-20.4	ELP-15A	-186.0	ELP-26	0.4
ELP-04 EW	24.5	ELP-08	-22.0	ELP-15A	-186.8	ELP-27	0.8
ELP-04 LW	24.0	ELP-09 EW	-22.1	ELP-05	-173.7	ELP-28	0.5
ELP-05	23.2	ELP-09 LW	-22.3	ELP-16A	-184.7	ELP-29	0.9
ELP-05	21.8	ELP-20	-22.3	ELP-16A	-186.3	ELP-30	0.8
ELP-05	23.9	ELP-21	-22.5	ELP-06	-182.2	ELP-31	1
ELP-06	22.0	ELP-22	-22.3	ELP-08	-184.3	ELP-32	1.5
ELP-06	22.3	ELP-23	-22.5	ELP-09	-177.6	ELP-33	1.2
ELP-06	21.9	ELP-24	-22.3	ELP-20	-159.0	ELP-34	0.7
ELP-07	22.4	ELP-25	-22.0	ELP-22	-159.0	ELP-35	0.5
ELP-07	21.9	ELP-26	-21.8			ELP-36	0.6
ELP-08	21.8	ELP-27	-21.7	ELP-26	-164.8	ELP-37	0.8
ELP-08	21.3	ELP-28	-21.8	ELP-28	-187.5	ELP-38	1
ELP-08	22.5	ELP-29	-22.8	ELP-29	-188.0	ELP-39	0.9
ELP-09 EW	21.0	ELP-30	-22.9	ELP-30	-164.8	ELP-40	1
ELP-09 EW	21.3	ELP-31	-23.0	ELP-31	-156.8	ELP-41	0.5

ELP-09 EW	21.6	ELP-32 EW	-22.8	ELP-32EW	-180.4	ELP-42	0.4
ELP-09 LW	20.2	ELP-32 LW	-23.9	ELP-33	-188.8	ELP-43	0.8
ELP-09 LW	20.0	ELP-33	-23.8	ELP-34EW	-179.0	ELP-44	0.7
ELP-20	20.7	ELP-34 EW	-23.7	ELP-34LW	-166.0	ELP-45	0.4
ELP-20	20.2	ELP-34 LW	-23.0	ELP-36	-171.9	ELP-46	0.6
ELP-21	20.2	ELP-35	-22.6			ELP-47	0.7
ELP-21	19.9	ELP-36	-22.3	ELP-41	-184.3	ELP-48	0.6
ELP-22	20.4	ELP-37	-22.9	ELP-42	-190.7	ELP-49	0.8
ELP-22	20.1	ELP-38	-23.6	ELP-43	-183.6	ELP-50	0.9
ELP-22	20.7	ELP-39	-23.5	ELP-44EW	-188.8	ELP-51	0.6
ELP-23	20.5	ELP-40	-22.8	ELP-44LW	-175.6	ELP-52	0.5
ELP-23	20.1	ELP-41	-22.1	ELP-45	-172.0	ELP-53	0.6
ELP-23	20.0	ELP-42	-22.4	ELP-46	-166.0	ELP-54	0.7
ELP-24	22.6	ELP-43	-22.5	ELP-47	-174.7	ELP-55	0.2
ELP-24	22.0	ELP-44EW	-22.3	ELP-48	-183.0	ELP-56	0.5
ELP-25	22.9	ELP-44LW	-22.0	ELP-49EW	-179.5	ELP-57	0.3
ELP-26		ELP-45	-21.6	ELP-49LW	-168.9	ELP-58	0.5
ELP-26	21.0	ELP-46	-22.1	ELP-50	-172.4	ELP-59	1
ELP-27		ELP-47	-21.9	ELP-52	-165.1	ELP-60	1.1
ELP-27	22.2	ELP-48	-22.4	ELP-53	-161.2	ELP-61	0.8
ELP-27	21.6	ELP-49 EW	-21.8			ELP-62	0.7
ELP-28		ELP-49 LW	-21.8	ELP-57	-176.1	ELP-63	1.2
ELP-28	23.3	ELP-50	-21.6	ELP-58EW	-168.8	ELP-64	1.1
ELP-28	24.2	ELP-51	-22.1	ELP-58LW	-167.7	ELP-65	1.5
ELP-29	23.0	ELP-52	-23.0	ELP-59	-166.3	ELP-66	1.3
ELP-29	23.0	ELP-53	-22.6	ELP-60	-176.5	ELP-67	1
ELP-30		ELP-54	-23.4	ELP-61LW	-165.1	ELP-68	0.9
ELP-30	22.9	ELP-55	-22.7	ELP-62	-173.3	ELP-69	0.8
ELP-31	17.9	ELP-56		ELP-63EW	-165.1	ELP-70	0.5
ELP-32 EW	22.2	ELP-57	-22.0	ELP-63LW	-177.4	ELP-71	0.6
ELP-32 EW	22.2	ELP-58 EW	-21.5	ELP-64LW	-173.4	ELP-72	0.8
ELP-32 EW	22.8	ELP-58 LW	-22.0			ELP-73	0.9
ELP-32 LW	21.0	ELP-59	-21.7	ELP-69LW	-185.3	ELP-74	1
ELP-33	22.4	ELP-60	-22.2	ELP-69LW	-187.8	ELP-75	0.8
ELP-33		ELP-61 EW	-22.3	ELP-70	-160.0	ELP-76	0.4
ELP-33	21.5	ELP-61 LW	-22.4	ELP-71	-175.8	ELP-77	0.5
ELP-34 EW		ELP-62	-22.2	ELP-71	-169.2	ELP-78	0.7
ELP-34 EW	21.9	ELP-63 EW	-21.5	ELP-75	-173.7	ELP-79	1
ELP-34 EW	21.7	ELP-63 LW	-21.8	ELP-75	-180.0	ELP-80	1
ELP-34 LW	23.3	ELP-64 LW	-21.5	ELP-77	-173.2	ELP-81	0.4
ELP-34 LW		ELP-65	-21.2	ELP-77	-164.8	ELP-82	0.3
ELP-34 LW	23.7	ELP-66	-21.7	ELP-78	-188.4	ELP-83	0.2
ELP-35	22.5	ELP-67	-22.3	ELP-78	-182.9	ELP-84	0.1
ELP-35	22.6	ELP-68	-21.6	ELP-79	-137.2	ELP-85	0.05
ELP-36	23.3	ELP-69 EW	-22.4	ELP-79	-88.4	ELP-86	0.1

ELP-36	22.5	ELP-69 LW	-22.2	ELP-80	-177.9	ELP-87	0.2
ELP-37	17.5	ELP-70	-22.3	ELP-80	-182.2	ELP-88	0.4
ELP-38	17.3	ELP-71	-22.5	ELP-81	-192.9	ELP-89	0.1
ELP-39	16.4	ELP-72	-13.4	ELP-81	-188.9	ELP-90	0.1
ELP-40	20.2	ELP-73	-23.3	ELP-83	-169.1	ELP-91	0.2
ELP-41	19.3	ELP-74	-22.3	ELP-84	-183.1	ELP-92	0.1
ELP-42	17.5	ELP-75	-21.5	ELP-84	-181.3	ELP-93	0.1
ELP-43	17.2	ELP-76	-22.0	ELP-86	-180.2	ELP-94	0.2
ELP-44 EW	14.7	ELP-77	-21.8	ELP-87	-184.1	ELP-95	0.2
ELP-44 LW	18.2	ELP-78	-21.9	ELP-87	-170.1	ELP-96	0.3
ELP-45	17.4	ELP-79	-21.8	ELP-92	-56.9	ELP-97	0.2
ELP-46	18.2	ELP-80	-21.7	ELP-94	-191.6	ELP-98	0.2
ELP-47	19.1	ELP-81	-22.6	ELP-94	-188.9	ELP-99	0.1
ELP-48	19.9	ELP-82	-22.4	ELP-95	-196.9	ELP-100	0.2
ELP-49 EW	19.7	ELP-83	-22.4	ELP-95	-197.0	ELP-101	0.1
ELP-49 LW	19.0	ELP-84	-21.2	ELP-96	-188.1	ELP-102	0.05
ELP-50	17.7	ELP-85	-21.0	ELP-97	-172.6	ELP-103	0.1
ELP-51	18.2	ELP-86	-21.2	ELP-98	-205.2	ELP-104	0.1
ELP-52	16.5	ELP-87	-22.4	ELP-98	-203.2	ELP-105	0.2
ELP-53	18.2	ELP-88	-21.4	ELP-99	-204.1	ELP-106	0.1
ELP-54	19.8	ELP-89	-21.7	ELP-99	-204.9	ELP-107	0.2
ELP-55	17.6	ELP-90		ELP-100	-199.6	ELP-108	0.4
ELP-56	20.2	ELP-91		ELP-100	-200.2	ELP-109	0.3
ELP-57	18.2	ELP-92	-21.4	ELP-101	-198.0	ELP-110	0.3
ELP-58 EW	19.9	ELP-93	-22.2	ELP-101	-190.4	ELP-111	0.4
ELP-58 LW	18.9	ELP-94	-22.1	ELP-102	-195.1	ELP-112	0.1
ELP-59	19.4	ELP-95	-22.2	ELP-102	-193.6	ELP-113	0.2
ELP-60	19.5	ELP-96		ELP-103	-190.8	ELP-114	0.2
ELP-61 EW	18.8	ELP-97	-17.7	ELP-103	-196.0	ELP-115	0.1
ELP-61 LW	18.9	ELP-98	-21.9	ELP-104	-198.5	ELP-116	0.2
ELP-62	17.4	ELP-99	-22.2	ELP-104	-198.3	ELP-117	0.1
ELP-63 EW	19.1	ELP-100	-22.6	ELP-105	-199.8	ELP-118	0.3
ELP-63 LW	17.5	ELP-101	-22.2	ELP-105	-192.3	ELP-119	0.3
ELP-64 LW	18.4	ELP-102	-22.9	ELP-106	-192.6	ELP-120	0.2
ELP-65	18.3	ELP-103	-22.7	ELP-107	-195.5	ELP-121	0.3
ELP-66	18.7	ELP-104	-22.9	ELP-107	-190.2	ELP-122	0.1
ELP-67	16.7	ELP-105	-22.1	ELP-108	-188.0	ELP-123	0.2
ELP-68	17.9	ELP-106	-22.4	ELP-108	-190.8	ELP-124	0.2
ELP-69 EW	17.1	ELP-107	-23.5	ELP-109	-190.6	ELP-125	0.3
ELP-69 LW	16.9	ELP-108	-22.2	ELP-109	-195.2	ELP-126	0.2
ELP-70	17.4	ELP-109	-22.2	ELP-111	-145.4	ELP-127	0.1
ELP-71	17.2	ELP-110	-23.5	ELP-113	-189.9	ELP-128	0.1
ELP-72		ELP-111	-23.0	ELP-113	-191.6	ELP-129	0.2
ELP-73	17.7	ELP-112	-22.5	ELP-115	-182.6	ELP-130	0.1
ELP-74	20.7	ELP-113	-22.7	ELP-115	-185.0	ELP-131	0.2

ELP-75	20.8	ELP-114	-22.6	ELP-119	-172.9	ELP-132	0.3
ELP-76	19.1	ELP-115	-22.5	ELP-119	-179.5	ELP-133	0.4
ELP-77	19.0	ELP-116	-22.7	ELP-120	-178.2	ELP-134	0.3
ELP-78	17.5	ELP-117	-22.9	ELP-120	-141.6	ELP-135	0.5
ELP-79	18.1	ELP-118	-23.1	ELP-121	-178.3	ELP-136	0.2
ELP-80	18.7	ELP-119	-22.0	ELP-121	-179.1	ELP-137	0.4
ELP-81	18.5	ELP-120	-22.4	ELP-122	-179.5	ELP-138	0.3
ELP-82	17.0	ELP-121	-22.4	ELP-122	-176.5	ELP-139	0.4
ELP-83	19.9	ELP-122	-22.1	ELP-123	-177.9	ELP-140	0.4
ELP-84	20.1	ELP-123	-22.4	ELP-123	-180.3	ELP-141	0.5
ELP-85	17.6	ELP-124	-22.7	ELP-125	-171.6	ELP-142	0.4
ELP-86	19.1	ELP-125	-22.6	ELP-126	-185.9	ELP-143	0.3
ELP-87	17.5	ELP-126	-22.2	ELP-126	-185.8	ELP-144	0.4
ELP-88	20.9	ELP-127	-22.5	ELP-127	-175.3	ELP-145	0.2
ELP-89	19.4	ELP-128	-23.2	ELP-127	-177.8	ELP-146	0.4
ELP-90	18.7	ELP-129	-22.8	ELP-128	-175.4	ELP-147	0.3
ELP-91	20.1	ELP-130	-22.5	ELP-129	-184.5	ELP-148	0.4
ELP-92	19.6	ELP-131	-22.4	ELP-129	-177.9	ELP-149	0.4
ELP-93	18.6	ELP-132	-22.3	ELP-130	-182.9	ELP-150	0.5
ELP-94	17.9	ELP-133	-22.5	ELP-130	-186.3	ELP-151	0.6
ELP-95	17.2	ELP-134	-22.7	ELP-131	-139.0	ELP-152	0.4
ELP-96	17.6	ELP-135	-22.4	ELP-135	-194.4	ELP-153	0.3
ELP-97	19.7	ELP-136	-23.0	ELP-135	-189.9	ELP-154	0.2
ELP-98	19.4	ELP-137	-22.5	ELP-136	-187.3	ELP-155	0.1
ELP-99	18.3	ELP-138	-21.1	ELP-136	-190.7	ELP-156	0.1
ELP-100	18.9	ELP-139	-21.8	ELP-138	-185.7	ELP-157	0.05
ELP-101	20.1	ELP-140	-21.6	ELP-139		ELP-158	0.1
ELP-102	19.3	ELP-141	-20.8	ELP-140		ELP-159	0.1
ELP-103	19.2	ELP-142	-21.0	ELP-141		ELP-160	0.1
ELP-104	18.5	ELP-143	-21.1	ELP-142	-178.7	ELP-161	0.1
ELP-105	19.9	ELP-144	-20.6	ELP-142	-180.7	ELP-162	0.2
ELP-106	19.5	ELP-145	-21.2	ELP-143	-182.0	ELP-163	0.1
ELP-107	20.3	ELP-146	-21.0	ELP-143	-181.4	ELP-164	0.2
ELP-108	19.8	ELP-147	-22.0	ELP-145	-180.1	ELP-165	0.3
ELP-109	19.1	ELP-148	-21.7	ELP-145	-185.2	ELP-166	0.2
ELP-110	19.0	ELP-149	-22.1	ELP-147	-191.3	ELP-167	0.1
ELP-111	19.2	ELP-150	-22.2	ELP-148	-184.9	ELP-168	0.2
ELP-112	19.4	ELP-151 EW	-21.6	ELP-150	-188.3	ELP-169	0.2
ELP-113	19.3	ELP-151 LW	-21.0	ELP-150	-173.4	ELP-170	0.4
ELP-114	19.5	ELP-152	-21.2	ELP-151 EW	-183.8	ELP-171	0.3
ELP-115	18.9	ELP-153	-22.1	ELP-151 EW	-185.2	ELP-172	0.1
ELP-116	18.7	ELP-154	-21.8	ELP-151 LW	-179.5	ELP-173	0.2
ELP-117	18.7	ELP-155	-21.9	ELP-151 LW	-183.8	ELP-174	0.1
ELP-118		ELP-156	-22.0	ELP-152	-183.6	ELP-175	0.2
ELP-119		ELP-157	-22.2	ELP-152	-184.3	ELP-176	0.2

ELP-120	19.6	ELP-158	-22.3	ELP-153	-184.8	ELP-177	0.1
ELP-121	19.6	ELP-158 FR	-21.9	ELP-153	-179.5	ELP-178	0.1
ELP-122	19.5	ELP-159 EW	-21.6	ELP-154	-184.9	ELP-179	0.2
ELP-123	18.7	ELP-159 LW	-22.1	ELP-154	-185.5	ELP-180	0.1
ELP-124	19.3	ELP-160	-22.2	ELP-156	-191.7	ELP-181	0.2
ELP-125	18.9	ELP-161	-22.5	ELP-157	-188.7	ELP-182	0.2
ELP-126	18.9	ELP-162	-22.7	ELP-157	-182.9	ELP-183	0.1
ELP-127	18.7	ELP-163	-22.8	ELP-158	-187.7	ELP-184	0.1
ELP-128	19.2	ELP-164	-22.8	ELP-159EW	-175.4	ELP-185	0.1
ELP-129	18.9	ELP-165	-22.7	ELP-159EW	-176.1	ELP-186	0.05
ELP-130	19.2	ELP-166	-22.7	ELP-160	-174.9	ELP-187	0.06
ELP-131	19.5	ELP-167	-22.6	ELP-161	-179.4	ELP-188	0.07
ELP-132	19.3	ELP-168 EW	-22.6	ELP-162	-189.9	ELP-189	0.1
ELP-133	18.6	ELP-168 LW	-22.5	ELP-162	-191.9	ELP-190	0.1
ELP-134	19.0	ELP-169	-22.5	ELP-163	-185.7	ELP-191	0.05
ELP-135	19.1	ELP-170	-22.3	ELP-163	-184.6	ELP-192	0.2
ELP-136	19.4	ELP-171	-22.2	ELP-164	-178.2	ELP-193	0.1
ELP-137	20.5	ELP-172	-22.5	ELP-164	-180.8	ELP-194	0.1
ELP-138	21.6	ELP-173	-23.4	ELP-165	-191.0	ELP-195	0.2
ELP-139	20.3	ELP-174	-20.9	ELP-165	-191.1	ELP-196	0.1
ELP-140	20.5	ELP-175	-22.0	ELP-166	-187.4	ELP-197	0.1
ELP-141	19.2	ELP-176	-21.9	ELP-166	-190.1	ELP-198	0.2
ELP-142	20.4	ELP-177	-22.0	ELP-167	-193.3	ELP-199	0.2
ELP-143	20.1	ELP-178 EW	-21.3	ELP-167	-195.0	ELP-200	0.1
ELP-144	20.7	ELP-178 LW	-21.3	ELP-168EW	-194.9	ELP-201	0.1
ELP-145	21.7	ELP-179	-20.8	ELP-168EW	-192.4	ELP-202	0.2
ELP-146	20.6	ELP-180	-21.2	ELP-168LW	-188.3	ELP-203	0.1
ELP-147	19.2	ELP-181	-21.1	ELP-168LW	-189.4		
ELP-148	19.5	ELP-182 EW	-21.1	ELP-169			
ELP-149	19.5	ELP-182 LW	-21.3	ELP-169	-187.8		
ELP-150	17.8	ELP-183	-20.7	ELP-170	-187.9		
ELP-151 EW	20.5	ELP-184	-20.9	ELP-170	-189.6		
ELP-151 LW	21.4	ELP-185	-20.8	ELP-171	-186.9		
ELP-152	21.2	ELP-186	-21.5	ELP-171	-188.0		
ELP-153	19.8	ELP-187	-22.4	ELP-172	-180.4		
ELP-154	19.8	ELP-188	-21.3	ELP-172	-150.4		
ELP-155	19.8	ELP-189	-21.7	ELP-173	-191.2		
ELP-156	18.2	ELP-190	-21.3	ELP-173	-191.8		
ELP-157	17.7	ELP-191	-22.0	ELP-174	-180.5		
ELP-158	17.7	ELP-192	-21.9	ELP-174	-192.2		
ELP-158 FR	18.6	ELP-193	-22.7	ELP-175	-183.4		
ELP-159 EW	18.4	ELP-194	-21.2	ELP-175	-187.8		
ELP-159 LW	18.0	ELP-195	-21.6	ELP-176	-183.9		
ELP-160	18.1	ELP-196	-21.6	ELP-176	-187.4		
ELP-161	17.7	ELP-197	-22.2	ELP-177	-187.0		

ELP-162	17.9	ELP-198	-22.4	ELP-178EW	-186.3		
ELP-163	18.1	ELP-199	-22.5	ELP-178LW	-184.5		
ELP-164	18.5	ELP-200	-22.9	ELP-180	-190.9		
ELP-165	19.0	ELP-201	-23.0	ELP-181	-194.2		
ELP-166	19.3	ELP-202	-23.1	ELP-181	-190.0		
ELP-167	18.8	ELP-203	-22.6	ELP-181	-182.2		
ELP-168 EW	19.0			ELP-182EW	-178.6		
ELP-168 LW	19.6			ELP-182LW	-171.8		
ELP-169	20.3			ELP-183	-162.3		
ELP-170	20.6			ELP-183	-182.4		
ELP-171	16.6			ELP-184	-171.1		
ELP-172	20.0			ELP-184	-177.0		
ELP-173	18.0			ELP-185	-169.0		
ELP-174	18.1			ELP-186	-166.3		
ELP-175	18.9			ELP-188	-169.3		
ELP-176	18.9			ELP-189	-168.1		
ELP-177	18.6			ELP-190	-185.5		
ELP-178 EW	18.3			ELP-191	-180.4		
ELP-178 LW	18.9			ELP-192	-182.9		
ELP-179				ELP-193	-179.9		
ELP-180	18.5			ELP-194	-180.6		
ELP-181	19.0			ELP-195	-186.9		
ELP-182 EW	19.5			ELP-196	-178.4		
ELP-183 LW	18.3			ELP-197	-181.9		
ELP-183	20.2			ELP-198	-185.6		
ELP-184				ELP-199	-182.0		
ELP-185				ELP-200	-187.6		
ELP-186	21.1			ELP-201	-180.2		
ELP-187	19.5			ELP-202	-190.3		
ELP-188	19.9			ELP-203	-183.4		
ELP-189	19.6						
ELP-190	18.3						
ELP-191	19.1						
ELP-192	17.9						
ELP-193	18.9						
ELP-194	19.6						
ELP-195	20.2						
ELP-196	19.9						
ELP-197	20.5						
ELP-198	20.3						
ELP-199	19.9						
ELP-200	18.7						
ELP-201	18.5						
ELP-202	18.7						
ELP-203	18.0						

Appendix B:

Source water and temperature calculations using the Roden *et al.* 2000 and Anderson *et al.* 2002 equations

Calculations using the Anderson *et al*., 2002 equation

Ring	d18O	humidity	Ee	alpha	Ek	f	Ebiochem	dsw	Temperature
1	15.92	0.7	10.24	1.01	28	0.2	27	-21.79	14.4
2	19.45	0.7	10.24					-18.26	14.4
3	21.52	0.7	10.24					-16.18	14.4
3.5	20.77	0.7	10.24					-16.93	14.4
4	21.29	0.7	10.24					-16.42	14.4
5	20.56	0.7	10.24					-17.15	14.4
6	20.36	0.7	10.24					-17.35	14.4
7	20.77	0.7	10.24					-16.94	14.4
8	21.77	0.7	10.24					-15.94	14.4
9	22.45	0.7	10.24					-15.26	14.4
10	20.58	0.7	10.24					-17.13	14.4
11	20.62	0.7	10.24					-17.09	14.4
12	21.02	0.7	10.24					-16.69	14.4
12.5	21.14	0.7	10.24					-16.57	14.4
13	22.81	0.7	10.24					-14.90	14.4
13.5	23.39	0.7	10.24					-14.32	14.4
14	24.46	0.7	10.24					-13.25	14.4
14.5	23.99	0.7	10.24					-13.72	14.4
15	22.96	0.7	10.24					-14.74	14.4
16	22.08	0.7	10.24					-15.63	14.4
17	22.15	0.7	10.24					-15.56	14.4
18	21.87	0.7	10.24					-15.84	14.4
19	21.30	0.7	10.24					-16.41	14.4
19.5	20.08	0.7	10.24					-17.63	14.4
20	20.45	0.7	10.24					-17.26	14.4
21	20.04	0.7	10.24					-17.66	14.4
22	20.41	0.7	10.24					-17.30	14.4
23	20.20	0.7	10.24					-17.51	14.4
24	22.33	0.7	10.24					-15.38	14.4
25	22.91	0.7	10.24					-14.80	14.4
26	20.98	0.7	10.24					-16.72	14.4
27	21.90	0.7	10.24					-15.81	14.4
28	23.75	0.7	10.24					-13.95	14.4
29	23.04	0.7	10.24					-14.67	14.4
30	22.87	0.7	10.24					-14.84	14.4
31	17.86	0.7	10.24					-19.85	14.4
32	20.74	0.7	10.24					-16.96	14.4
32.5	20.98	0.7	10.24					-16.73	14.4
33	21.71	0.7	10.24					-16.00	14.4
34	21.72	0.7	10.24					-15.99	14.4
34.5	22.51	0.7	10.24					-15.20	14.4
35	23.09	0.7	10.24					-14.62	14.4
36	22.95	0.7	10.24					-14.75	14.4
37	17.53	0.7	10.24					-20.17	14.4
38	17.28	0.7	10.24					-20.43	14.4
39	16.40	0.7	10.24					-21.30	14.4
40	20.21	0.7	10.24					-17.49	14.4
41	19.32	0.7	10.24					-18.39	14.4
42	17.54	0.7	10.24					-20.17	14.4
43	17.19	0.7	10.24					-20.52	14.4
44	14.70	0.7	10.24					-23.01	14.4
44.5	18.19	0.7	10.24					-19.52	14.4
45	17.44	0.7	10.24					-20.26	14.4
46	18.18	0.7	10.24					-19.53	14.4
47	19.05	0.7	10.24					-18.66	14.4
48	19.94	0.7	10.24					-17.77	14.4
49	19.74	0.7	10.24					-17.96	14.4

49.5	19.04	0.7	10.24					-18.67	14.4
50	17.66	0.7	10.24					-20.05	14.4
51	18.17	0.7	10.24					-19.53	14.4
52	16.51	0.7	10.24					-21.20	14.4
53	18.17	0.7	10.24					-19.54	14.4
54	19.81	0.7	10.24					-17.90	14.4
55	17.63	0.7	10.24					-20.07	14.4
56	20.18	0.7	10.24					-17.53	14.4
57	18.15	0.7	10.24					-19.55	14.4
58	19.94	0.7	10.24					-17.77	14.4
58.5	18.86	0.7	10.24					-18.85	14.4
59	19.38	0.7	10.24					-18.33	14.4
60	19.46	0.7	10.24					-18.24	14.4
61	18.78	0.7	10.24					-18.92	14.4
61.5	18.91	0.7	10.24					-18.80	14.4
62	17.43	0.7	10.24					-20.28	14.4
63	19.13	0.7	10.24					-18.58	14.4
63.5	17.50	0.7	10.24					-20.21	14.4
64.5	18.42	0.7	10.24					-19.29	14.4
65	18.29	0.7	10.24					-19.41	14.4
66	18.74	0.7	10.24					-18.97	14.4
67	16.75	0.7	10.24					-20.96	14.4
68	17.88	0.7	10.24					-19.83	14.4
69	17.06	0.7	10.24					-20.64	14.4
69.5	16.91	0.7	10.24					-20.79	14.4
70	17.38	0.7	10.24					-20.33	14.4
71	17.20	0.7	10.24					-20.50	14.4
73	17.70	0.7	10.24					-20.01	14.4
74	20.68	0.7	10.24					-17.03	14.4
75	20.79	0.7	10.24					-16.92	14.4
76	19.09	0.7	10.24					-18.62	14.4
77	18.99	0.7	10.24					-18.72	14.4
78	17.54	0.7	10.24					-20.17	14.4
79	18.12	0.7	10.24					-19.58	14.4
80	18.66	0.7	10.24					-19.05	14.4
81	18.47	0.7	10.24					-19.24	14.4
82	17.04	0.7	10.24					-20.66	14.4
83	19.86	0.7	10.24					-17.85	14.4
84	20.11	0.7	10.24					-17.60	14.4
85	17.56	0.7	10.24					-20.15	14.4
86	19.12	0.7	10.24					-18.59	14.4
87	17.48	0.7	10.24					-20.22	14.4
88		0.7	10.24						14.4
89	19.39	0.7	10.24					-18.31	14.4
90	18.70	0.7	10.24					-19.01	14.4
91	20.09	0.7	10.24					-17.62	14.4
92	19.60	0.7	10.24					-18.11	14.4
93	18.55	0.7	10.24					-19.15	14.4
94	17.92	0.7	10.24					-19.78	14.4
95	17.17	0.7	10.24					-20.54	14.4
96	17.63	0.7	10.24					-20.08	14.4
97	19.68	0.7	10.24					-18.02	14.4
98	19.38	0.7	10.24					-18.33	14.4
99	18.33	0.7	10.24					-19.38	14.4
100	18.86	0.7	10.24					-18.84	14.4
101	20.07	0.7	10.24					-17.64	14.4
102	19.34	0.7	10.24					-18.37	14.4
103	19.16	0.7	10.24					-18.54	14.4
104	18.51	0.7	10.24					-19.19	14.4
105	19.88	0.7	10.24					-17.83	14.4
106	19.50	0.7	10.24					-18.21	14.4

107	20.27	0.7	10.24					-17.43	14.4
108	19.82	0.7	10.24					-17.89	14.4
109	19.08	0.7	10.24					-18.63	14.4
110	18.97	0.7	10.24					-18.74	14.4
111	19.23	0.7	10.24					-18.47	14.4
112	19.36	0.7	10.24					-18.35	14.4
113	19.30	0.7	10.24					-18.41	14.4
114	19.47	0.7	10.24					-18.23	14.4
115	18.86	0.7	10.24					-18.85	14.4
116	18.67	0.7	10.24					-19.04	14.4
117	18.74	0.7	10.24					-18.96	14.4
120	19.60	0.7	10.24					-18.11	14.4
121	19.60	0.7	10.24					-18.11	14.4
122	19.48	0.7	10.24					-18.22	14.4
123	18.73	0.7	10.24					-18.98	14.4
124	19.34	0.7	10.24					-18.37	14.4
125	18.89	0.7	10.24					-18.81	14.4
126	18.94	0.7	10.24					-18.77	14.4
127	18.70	0.7	10.24					-19.00	14.4
128	19.18	0.7	10.24					-18.52	14.4
129	18.91	0.7	10.24					-18.79	14.4
130	19.20	0.7	10.24					-18.51	14.4
131	19.47	0.7	10.24					-18.24	14.4
132	19.27	0.7	10.24					-18.44	14.4
133	18.62	0.7	10.24					-19.09	14.4
134	18.96	0.7	10.24					-18.74	14.4
135	19.11	0.7	10.24					-18.60	14.4
136	19.36	0.7	10.24					-18.35	14.4
137	20.49	0.7	10.24					-17.22	14.4
138	21.56	0.7	10.24					-16.15	14.4
139	20.33	0.7	10.24					-17.38	14.4
140	20.46	0.7	10.24					-17.24	14.4
141	19.19	0.7	10.24					-18.52	14.4
142	20.42	0.7	10.24					-17.29	14.4
143	20.12	0.7	10.24					-17.59	14.4
144	20.70	0.7	10.24					-17.01	14.4
145	21.75	0.7	10.24					-15.96	14.4
146	20.64	0.7	10.24					-17.06	14.4
147	19.18	0.7	10.24					-18.53	14.4
148	19.55	0.7	10.24					-18.16	14.4
149	19.53	0.7	10.24					-18.17	14.4
150	17.77	0.7	10.24					-19.94	14.4
151	20.52	0.7	10.24					-17.19	14.4
151.5	21.44	0.7	10.24					-16.27	14.4
152	21.16	0.7	10.24					-16.55	14.4
153	19.83	0.7	10.24					-17.87	14.4
154	19.78	0.7	10.24					-17.93	14.4
155	19.79	0.7	10.24					-17.92	14.4
156	18.17	0.7	10.24					-19.54	14.4
157	17.74	0.7	10.24					-19.96	14.4
158	17.66	0.7	10.24					-20.05	14.4
158.5	18.58	0.7	10.24					-19.12	14.4
159	18.37	0.7	10.24					-19.34	14.4
159.5	18.04	0.7	10.24					-19.67	14.4
160	18.10	0.7	10.24					-19.61	14.4
161	17.71	0.7	10.24					-20.00	14.4
162	17.86	0.7	10.24					-19.84	14.4
163	18.10	0.7	10.24					-19.60	14.4
164	18.55	0.7	10.24					-19.16	14.4
165	19.01	0.7	10.24					-18.70	14.4
166	19.29	0.7	10.24					-18.42	14.4

167	18.77	0.7	10.24					-18.94	14.4
168	19.01	0.7	10.24					-18.70	14.4
168.5	19.59	0.7	10.24					-18.11	14.4
169	20.25	0.7	10.24					-17.46	14.4
170	20.58	0.7	10.24					-17.13	14.4
171	16.58	0.7	10.24					-21.12	14.4
172	20.04	0.7	10.24					-17.67	14.4
173	18.03	0.7	10.24					-19.67	14.4
174	18.06	0.7	10.24					-19.65	14.4
175	18.85	0.7	10.24					-18.86	14.4
176	18.90	0.7	10.24					-18.81	14.4
177	18.64	0.7	10.24					-19.06	14.4
178	18.33	0.7	10.24					-19.37	14.4
178.5	18.92	0.7	10.24					-18.78	14.4
179		0.7	10.24					-19.00	14.4
180	18.50	0.7	10.24					-19.21	14.4
181	18.97	0.7	10.24					-18.73	14.4
182	19.46	0.7	10.24					-18.24	14.4
182.5	18.29	0.7	10.24					-19.42	14.4
183	20.17	0.7	10.24					-17.54	14.4
184		0.7	10.24					-17.07	14.4
185		0.7	10.24					-17.66	14.4
186	21.10	0.7	10.24					-16.61	14.4
187	19.47	0.7	10.24					-18.24	14.4
188	19.93	0.7	10.24					-17.78	14.4
189	19.60	0.7	10.24					-18.11	14.4
190	18.34	0.7	10.24					-19.37	14.4
191	19.09	0.7	10.24					-18.61	14.4
192	17.92	0.7	10.24					-19.78	14.4
193	18.88	0.7	10.24					-18.83	14.4
194	19.57	0.7	10.24					-18.14	14.4
195	20.16	0.7	10.24					-17.55	14.4
196	19.90	0.7	10.24					-17.80	14.4
197	20.46	0.7	10.24					-17.25	14.4
198	20.33	0.7	10.24					-17.38	14.4
199	19.93	0.7	10.24					-17.78	14.4
200	18.73	0.7	10.24					-18.98	14.4
201	18.46	0.7	10.24					-19.25	14.4
202	18.71	0.7	10.24					-19.00	14.4
203	18.03	0.7	10.24					-19.68	14.4
								-18.26	

Ring	d18O	humidity	dsw	dD	d18Oxw	dDxw	Ee	Temperature
1	15.92	0.7	-18.7	-177.22	-21.81	-221.22	10.33	13.44
2	19.45			-177.22	-18.29	-221.22	10.33	13.44
3	21.52			-179.07	-16.21	-223.07	10.33	13.44
3.5	20.77			-181.39	-16.96	-225.39	10.33	13.44
4	21.29			-183.70	-16.45	-227.70	10.33	13.44
5	20.56			-181.96	-17.18	-225.96	10.33	13.44
6	20.36			-183.62	-17.37	-227.62	10.33	13.44
7	20.77			-180.65	-16.96	-224.65	10.33	13.44
8	21.77			-170.55	-15.96	-214.55	10.33	13.44
9	22.45			-172.12	-15.29	-216.12	10.33	13.44
10	20.58			-174.70	-17.16	-218.70	10.33	13.44
11	20.62			-182.25	-17.11	-226.25	10.33	13.44
12	21.02			-180.42	-16.71	-224.42	10.33	13.44
12.5	21.14			-153.61	-16.59	-197.61	10.33	13.44
13	22.81			-185.83	-14.93	-229.83	10.33	13.44
13.5	23.39			-189.17	-14.34	-233.17	10.33	13.44
14	24.46			-187.33	-13.27	-231.33	10.33	13.44
14.5	23.99			-186.87	-13.74	-230.87	10.33	13.44
15	22.96			-186.40	-14.77	-230.40	10.33	13.44
16	22.08			-184.37	-15.65	-228.37	10.33	13.44
17	22.15			-184.32	-15.58	-228.32	10.33	13.44
18	21.87			-184.27	-15.86	-228.27	10.33	13.44
19	21.30			-177.56	-16.43	-221.56	10.33	13.44
19.5	20.08			-168.29	-17.65	-212.29	10.33	13.44
20	20.45			-159.03	-17.29	-203.03	10.33	13.44
21	20.04			-159.03	-17.69	-203.03	10.33	13.44
22	20.41			-159.03	-17.33	-203.03	10.33	13.44
23	20.20			-160.46	-17.53	-204.46	10.33	13.44
24	22.33			-161.89	-15.40	-205.89	10.33	13.44
25	22.91			-163.32	-14.83	-207.32	10.33	13.44
26	20.98			-164.75	-16.75	-208.75	10.33	13.44
27	21.90			-176.15	-15.83	-220.15	10.33	13.44
28	23.75			-187.54	-13.98	-231.54	10.33	13.44
29	23.04			-187.95	-14.70	-231.95	10.33	13.44
30	22.87			-164.77	-14.87	-208.77	10.33	13.44
31	17.86			-156.79	-19.88	-200.79	10.33	13.44
32	20.74			-180.43	-16.99	-224.43	10.33	13.44
32.5	20.98			-184.59	-16.75	-228.59	10.33	13.44
33	21.71			-188.75	-16.02	-232.75	10.33	13.44
34	21.72			-179.03	-16.01	-223.03	10.33	13.44
34.5	22.51			-166.03	-15.22	-210.03	10.33	13.44
35	23.09			-168.97	-14.64	-212.97	10.33	13.44
36	22.95			-171.91	-14.78	-215.91	10.33	13.44
37	17.53			-173.17	-20.20	-217.17	10.33	13.44
38	17.28			-174.44	-20.45	-218.44	10.33	13.44
39	16.40			-175.70	-21.33	-219.70	10.33	13.44
40	20.21			-176.33	-17.52	-220.33	10.33	13.44
41	19.32			-176.96	-18.42	-220.96	10.33	13.44
42	17.54			-175.44	-20.19	-219.44	10.33	13.44
43	17.19			-184.31	-20.54	-228.31	10.33	13.44
44	14.70			-190.66	-23.03	-234.66	10.33	13.44
44.5	18.19			-183.60	-19.55	-227.60	10.33	13.44
45	17.44			-188.81	-20.29	-232.81	10.33	13.44
46	18.18			-175.55	-19.56	-219.55	10.33	13.44
47	19.05			-172.04	-18.68	-216.04	10.33	13.44
48	19.94			-165.99	-17.80	-209.99	10.33	13.44
49	19.74			-174.75	-17.99	-218.75	10.33	13.44
49.5	19.04			-182.96	-18.69	-226.96	10.33	13.44
50	17.66			-179.48	-20.07	-223.48	10.33	13.44
51	18.17			-174.19	-19.56	-218.19	10.33	13.44

52	16.51			-168.89	-21.23	-212.89	10.33	13.44
53	18.17			-172.42	-19.56	-216.42	10.33	13.44
54	19.81			-173.35	-17.92	-217.35	10.33	13.44
55	17.63			-174.28	-20.10	-218.28	10.33	13.44
56	20.18			-175.21	-17.55	-219.21	10.33	13.44
57	18.15			-176.14	-19.58	-220.14	10.33	13.44
58	19.94			-168.75	-17.80	-212.75	10.33	13.44
58.5	18.86			-167.68	-18.87	-211.68	10.33	13.44
59	19.38			-166.33	-18.35	-210.33	10.33	13.44
60	19.46			-176.51	-18.27	-220.51	10.33	13.44
61	18.78			-170.81	-18.95	-214.81	10.33	13.44
61.5	18.91			-165.10	-18.82	-209.10	10.33	13.44
62	17.43			-173.30	-20.30	-217.30	10.33	13.44
63	19.13			-165.10	-18.61	-209.10	10.33	13.44
63.5	17.50			-177.43	-20.24	-221.43	10.33	13.44
64.5	18.42			-173.42	-19.32	-217.42	10.33	13.44
65	18.29			-176.69	-19.44	-220.69	10.33	13.44
66	18.74			-178.33	-18.99	-222.33	10.33	13.44
67	16.75			-179.96	-20.99	-223.96	10.33	13.44
68	17.88			-183.24	-19.85	-227.24	10.33	13.44
69	17.06			-184.88	-20.67	-228.88	10.33	13.44
69.5	16.91			-186.51	-20.82	-230.51	10.33	13.44
70	17.38			-160.03	-20.35	-204.03	10.33	13.44
71	17.20			-172.47	-20.53	-216.47	10.33	13.44
73	17.70			-174.65	-20.03	-218.65	10.33	13.44
74	20.68			-175.74	-17.06	-219.74	10.33	13.44
75	20.79			-176.83	-16.94	-220.83	10.33	13.44
76	19.09			-172.91	-18.65	-216.91	10.33	13.44
77	18.99			-168.98	-18.74	-212.98	10.33	13.44
78	17.54			-185.61	-20.20	-229.61	10.33	13.44
79	18.12			-182.82	-19.61	-226.82	10.33	13.44
80	18.66			-180.04	-19.07	-224.04	10.33	13.44
81	18.47			-190.89	-19.26	-234.89	10.33	13.44
82	17.04			-169.08	-20.69	-213.08	10.33	13.44
83	19.86			-182.20	-17.88	-226.20	10.33	13.44
84	20.11			-181.21	-17.63	-225.21	10.33	13.44
85	17.56			-180.71	-20.17	-224.71	10.33	13.44
86	19.12			-180.22	-18.62	-224.22	10.33	13.44
87	17.48			-184.14	-20.25	-228.14	10.33	13.44
88	18.44			-187.19	-19.29	-231.19	10.33	13.44
89	19.39			-188.72	-18.34	-232.72	10.33	13.44
90	18.70			-189.48	-19.03	-233.48	10.33	13.44
91	20.09			-190.24	-17.64	-234.24	10.33	13.44
92	19.60			-196.96	-18.14	-240.96	10.33	13.44
93	18.55			-188.10	-19.18	-232.10	10.33	13.44
94	17.92			-172.64	-19.81	-216.64	10.33	13.44
95	17.17			-204.18	-20.56	-248.18	10.33	13.44
96	17.63			-204.49	-20.11	-248.49	10.33	13.44
97	19.68			-199.92	-18.05	-243.92	10.33	13.44
98	19.38			-194.21	-18.36	-238.21	10.33	13.44
99	18.33			-194.35	-19.40	-238.35	10.33	13.44
100	18.86			-193.36	-18.87	-237.36	10.33	13.44
101	20.07			-198.42	-17.67	-242.42	10.33	13.44
102	19.34			-199.76	-18.39	-243.76	10.33	13.44
103	19.16			-192.61	-18.57	-236.61	10.33	13.44
104	18.51			-195.53	-19.22	-239.53	10.33	13.44
105	19.88			-189.41	-17.85	-233.41	10.33	13.44
106	19.50			-195.24	-18.24	-239.24	10.33	13.44
107	20.27			-194.11	-17.46	-238.11	10.33	13.44
108	19.82			-192.99	-17.92	-236.99	10.33	13.44
109	19.08			-191.86	-18.65	-235.86	10.33	13.44

110	18.97			-190.73	-18.77	-234.73	10.33	13.44
111	19.23			-187.26	-18.50	-231.26	10.33	13.44
112	19.36			-183.79	-18.38	-227.79	10.33	13.44
113	19.30			-181.90	-18.43	-225.90	10.33	13.44
114	19.47			-180.01	-18.26	-224.01	10.33	13.44
115	18.86			-178.12	-18.88	-222.12	10.33	13.44
116	18.67			-176.23	-19.07	-220.23	10.33	13.44
117	18.74			-178.21	-18.99	-222.21	10.33	13.44
120	19.60			-178.69	-18.14	-222.69	10.33	13.44
121	19.60			-177.97	-18.14	-221.97	10.33	13.44
122	19.48			-179.11	-18.25	-223.11	10.33	13.44
123	18.73			-175.34	-19.01	-219.34	10.33	13.44
124	19.34			-171.56	-18.39	-215.56	10.33	13.44
125	18.89			-185.85	-18.84	-229.85	10.33	13.44
126	18.94			-176.53	-18.80	-220.53	10.33	13.44
127	18.70			-175.45	-19.03	-219.45	10.33	13.44
128	19.18			-184.51	-18.55	-228.51	10.33	13.44
129	18.91			-184.57	-18.82	-228.57	10.33	13.44
130	19.20			-186.47	-18.54	-230.47	10.33	13.44
131	19.47			-188.37	-18.27	-232.37	10.33	13.44
132	19.27			-190.26	-18.47	-234.26	10.33	13.44
133	18.62			-191.21	-19.12	-235.21	10.33	13.44
134	18.96			-192.16	-18.77	-236.16	10.33	13.44
135	19.11			-188.99	-18.62	-232.99	10.33	13.44
136	19.36			-187.32	-18.37	-231.32	10.33	13.44
137	20.49			-185.66	-17.24	-229.66	10.33	13.44
138	21.56			-184.67	-16.18	-228.67	10.33	13.44
139	20.33			-183.69	-17.41	-227.69	10.33	13.44
140	20.46			-181.68	-17.27	-225.68	10.33	13.44
141	19.19			-179.66	-18.54	-223.66	10.33	13.44
142	20.42			-181.72	-17.31	-225.72	10.33	13.44
143	20.12			-182.17	-17.61	-226.17	10.33	13.44
144	20.70			-182.61	-17.03	-226.61	10.33	13.44
145	21.75			-186.94	-15.99	-230.94	10.33	13.44
146	20.64			-191.26	-17.09	-235.26	10.33	13.44
147	19.18			-184.86	-18.56	-228.86	10.33	13.44
148	19.55			-182.83	-18.19	-226.83	10.33	13.44
149	19.53			-180.81	-18.20	-224.81	10.33	13.44
150	17.77			-184.53	-19.97	-228.53	10.33	13.44
151	20.52			-181.64	-17.22	-225.64	10.33	13.44
151.5	21.44			-183.94	-16.29	-227.94	10.33	13.44
152	21.16			-182.17	-16.58	-226.17	10.33	13.44
153	19.83			-185.17	-17.90	-229.17	10.33	13.44
154	19.78			-188.41	-17.95	-232.41	10.33	13.44
155	19.79			-191.65	-17.94	-235.65	10.33	13.44
156	18.17			-185.82	-19.56	-229.82	10.33	13.44
157	17.74			-187.71	-19.99	-231.71	10.33	13.44
158	17.66			-181.71	-20.07	-225.71	10.33	13.44
158.5	18.58			-175.72	-19.15	-219.72	10.33	13.44
159	18.37			-175.29	-19.37	-219.29	10.33	13.44
159.5	18.04			-174.86	-19.69	-218.86	10.33	13.44
160	18.10			-179.39	-19.64	-223.39	10.33	13.44
161	17.71			-190.90	-20.02	-234.90	10.33	13.44
162	17.86			-185.15	-19.87	-229.15	10.33	13.44
163	18.10			-179.46	-19.63	-223.46	10.33	13.44
164	18.55			-191.05	-19.19	-235.05	10.33	13.44
165	19.01			-188.77	-18.72	-232.77	10.33	13.44
166	19.29			-194.17	-18.44	-238.17	10.33	13.44
167	18.77			-193.66	-18.96	-237.66	10.33	13.44
168	19.01			-188.82	-18.72	-232.82	10.33	13.44
168.5	19.59			-187.77	-18.14	-231.77	10.33	13.44

169	20.25			-188.74	-17.48	-232.74	10.33	13.44
170	20.58			-187.47	-17.15	-231.47	10.33	13.44
171	16.58			-180.41	-21.15	-224.41	10.33	13.44
172	20.04			-191.50	-17.70	-235.50	10.33	13.44
173	18.03			-186.36	-19.70	-230.36	10.33	13.44
174	18.06			-185.61	-19.68	-229.61	10.33	13.44
175	18.85			-185.69	-18.88	-229.69	10.33	13.44
176	18.90			-186.96	-18.83	-230.96	10.33	13.44
177	18.64			-186.27	-19.09	-230.27	10.33	13.44
178	18.33			-184.52	-19.40	-228.52	10.33	13.44
178.5	18.92			-187.72	-18.81	-231.72	10.33	13.44
179	18.71			-190.93	-19.02	-234.93	10.33	13.44
180	18.50			-194.23	-19.24	-238.23	10.33	13.44
181	18.97			-178.62	-18.76	-222.62	10.33	13.44
182	19.46			-171.81	-18.27	-215.81	10.33	13.44
182.5	18.29			-182.39	-19.45	-226.39	10.33	13.44
183	20.17			-174.07	-17.56	-218.07	10.33	13.44
184	20.63			-169.00	-17.10	-213.00	10.33	13.44
185	20.05			-166.26	-17.68	-210.26	10.33	13.44
186	21.10			-167.79	-16.64	-211.79	10.33	13.44
187	19.47			-169.31	-18.27	-213.31	10.33	13.44
188	19.93			-168.11	-17.80	-212.11	10.33	13.44
189	19.60			-185.53	-18.14	-229.53	10.33	13.44
190	18.34			-180.37	-19.40	-224.37	10.33	13.44
191	19.09			-182.85	-18.64	-226.85	10.33	13.44
192	17.92			-179.86	-19.81	-223.86	10.33	13.44
193	18.88			-180.57	-18.86	-224.57	10.33	13.44
194	19.57			-186.85	-18.17	-230.85	10.33	13.44
195	20.16			-178.40	-17.58	-222.40	10.33	13.44
196	19.90			-181.87	-17.83	-225.87	10.33	13.44
197	20.46			-185.64	-17.27	-229.64	10.33	13.44
198	20.33			-182.03	-17.41	-226.03	10.33	13.44
199	19.93			-187.65	-17.80	-231.65	10.33	13.44
200	18.73			-180.23	-19.00	-224.23	10.33	13.44
201	18.46			-190.28	-19.28	-234.28	10.33	13.44
202	18.71			-183.41	-19.03	-227.41	10.33	13.44
203	18.03			-180.98	-19.70	-224.98	10.33	13.44
	19.44			-180.97	-18.29	-224.97		

Curriculum Vitae

Education

MSc University of Saskatchewan, 2006
Thesis entitled: Pliocene climate change on Ellesmere Island, Canada: Annual variability determined from stable isotopes of fossil wood
Advisors: J.F. Basinger and W.P. Patterson

BSc(hons) Dalhousie University, 2003
Honours thesis entitled: The late Cretaceous-early Tertiary polar forests of northwest Ellesmere Island, Nunavut, Canada: palaeobotany, palaeoecology and palaeoclimatology.
Advisor: H.J. Falcon-Lang

Employment

Teaching Assistant, Dept. of Geol. Sci. University of Saskatchewan 2003-present
Courses taught:
Geol. 408.3 Geological Mapping (II), Geol. 463.3 Petroleum Geology, Geol. 343.3 Facies Models, Geol. 246.3 Stratigraphy and Stratigraphic Palaeontology, Geol. 229.3 Introductory Geochemistry, Geol. 121.3 Introductory Geology and Geol. 122.3 Earth History.

Senior undergraduate laboratory technician, Cosmogenic Nuclide Exposure Facility (CNEF) Dalhousie University 2002-2003
Responsible for processing samples from whole rocks to pure quartz, assisting in sample collection, organized schedules of other undergraduate lab technicians and assigned tasks.

Student field assistant, Geological Survey of Canada June 2001-Aug. 2001
Acted as a field assistant to various members of the TGI Cape Breton work group. Mostly surficial mapping but also involved some bedrock mapping and some geophysical field work.

Honors and Awards

Department of Geological Sciences Award for best graduate student seminar 2006

University of Saskatchewan Graduate student fellowship, 2004-2006

Geological Society of America graduate student research award, 2004

Northern Scientific Training Program student research award, 2004

The Atlantic Universities Geological Conference Canadian Society of Petroleum

Geologists Award for best student paper, 2001

Research Interests

Palaeoclimatology, particularly pre-Quaternary global change; palaeobotany, palaeoecology and plant climate interactions.

Society Memberships

Geological Society of America
Geological Association of Canada

Volunteer Activities

- Treasurer of various student societies including: Geology Graduate Student Society, University of Saskatchewan, 2005-Present; Dalhousie Science Society, Dalhousie University, 2002-2003; Dawson Geology Club, Dalhousie University, 2000-2002.
- Volunteer with "Let's talk Science" a graduate student program supporting science education in schools.
- Officer with the 328 Royal Canadian Army Cadet Corps in Saskatoon: Primarily as Band instructor but also teaching classes in citizenship, orienteering and bushcraft.
- Cornet player with the University of Saskatchewan Concert Band
- Judge at the 2005 WIUGC conference held in Saskatoon

Publications

Articles

Csank, A.Z., Patterson, W.P., Basinger, J.F., Eglington, B.M. (*in review*) Tree-ring stable isotope evidence for decadal scale climate variability in the Early Pliocene Arctic. Geology.

Falcon-Lang, H. J., MacRae, R.A., **Csank, A. Z.** 2004. Palaeoecology of Late Cretaceous polar vegetation preserved in the Hansen Point Volcanics, NW Ellesmere Island, Canada Palaeogeography, Palaeoclimatology, Palaeoecology, 212 (1-2): 45-64.

Conference Abstracts

Csank, A.Z., Patterson, W.P. and Basinger, J.F. 2005. Climate variability in the Early Pliocene Canadian High Arctic: evidence from subseasonal $\delta^{18}O$, δD and $\delta^{13}C$ values of fossil wood. Earth Systems Processes 2 , GSA Specialty Meetings Abstracts with Programs (**1**) pp. 62.

Csank, A.Z., Patterson, W.P. and Basinger, J.F. 2005. Annual climate variability for the Pliocene on Ellesmere Island, Canadian Arctic Archipelago, recorded in $\delta^{18}O$ and $\delta^{13}C$ values of fossil wood. 35th Annual International Arctic Workshop, Program and Abstracts 2005. Canadian Circumpolar Institute. University of Alberta. pp. 27.

Falcon-Lang, H.J., **Csank, A.Z.**, Basinger, J.F. 2005. Our forested Arctic, Palaeoecological evolution of the Mesozoic to Cenozoic polar forests. 35th Annual International Arctic Workshop, Program and Abstracts 2005. Canadian Circumpolar Institute. University of Alberta. pp. 72.

Csank, A.Z., Basinger, J.F., and Patterson, W.P. 2004. A new high-resolution stable isotope record from Pliocene wood, Ellesmere Island, Nunavut, Canada. Geological Society of America Annual Meeting, Denver, CO

Csank, A.Z., Basinger, J.F., Patterson, W.P., 2004: A high-resolution stable isotope climate record derived from tree rings of Pliocene wood, Ellesmere Island, Nunavut. GAC-MAC 29, St. Catherines 2004

Csank, A.Z., 2003: A Late Cretaceous-earliest Tertiary polar forest: what fossil wood can tell us about past environmental changes. Program with abstracts 38th meeting NEGSA.

Csank, A.Z., Falcon-Lang, H.J., MacRae, R.A., 2002: Life and times of some Late Cretaceous-Early Tertiary polar forests from northwest Ellesmere Island, Arctic, Canada. Atlantic Geology, 38 (**1**) pp. 80.

Csank, A.Z., 2001: A Late Cretaceous polar forest from NW Ellesmere Island: implications for climate past and future. Atlantic Geology, 37 (**3**) pp. 198.